The Early Proterozoic Matachewan Large Igneous Province: Geochemistry, Petrogenesis, and Implications for Earth Evolution

T. Jake. R. Ciborowski*[1, 2], Andrew C. Kerr[2], Richard E. Ernst[3], Iain McDonald[2], Matthew J. Minifie[2], Stephen S. Harlan[4], Ian L. Millar[5]

[1] Earth and Ocean Sciences, School of Natural Sciences, National University of Ireland, Galway, Ireland
[2] School of Earth and Ocean Sciences, Cardiff University, Park Place, Cardiff, Wales, CF10 3AT, UK
[3] Department of Earth Sciences, Carleton University, 1125 Colonel Bay Drive, Ottawa, Ontario, K1S 5B6, Canada & Faculty of Geology and Geography, Tomsk State University, 36 Lenin Ave, Tomsk 634050
[4] National Science Foundation, 4201 Wilson Blvd., Arlington, VA 22230, USA
[5] NERC Isotope Geosciences Laboratory, Keyworth, Nottingham NG12 5GG, UK

* jake.ciborowski@nuigalway.ie

ABSTRACT

The Matachewan Large Igneous Province (LIP) is interpreted to have formed during the early stages of mantle plume-induced continental break-up in the early Proterozoic. When the Matachewan LIP is reconstructed to its original configuration with units from the Superior Craton and other formerly adjacent blocks (Karelia, Kola, Wyoming and Hearne), the dyke swarms, layered intrusions and flood basalts, emplaced over the lifetime of the province, comprise one of the most extensive magmatic provinces recognised in the geological record. New geochemical data allow, for the first time, the Matachewan LIP to be considered as a single, coherent entity and show that Matachewan LIP rocks share a common tholeiitic composition and trace element geochemistry, characterised by enrichment in the most incompatible elements and depletion in the less incompatible elements. This signature, ubiquitous in early Proterozoic continental magmatic rocks, may indicate that the Matachewan LIP formed through contamination of the primary magmas with lithospheric material or, that the early Proterozoic mantle had a fundamentally different composition to the modern mantle. In addition to the radiating geometry of the dyke swarms, a plume origin for the Matachewan LIP is consistent with the geochemistry of some of the suites; these suites are

used to constrain a source mantle potential temperature of approximately 1500-1550°C. Comparison of these mantle potential temperatures with estimated temperatures for the early Proterozoic upper mantle, are consistent with a hot mantle plume source for the magmatism. Geochemical data from coeval intrusions suggest that the plume head was compositionally heterogeneous and sampled material from both depleted and enriched mantle. As has been documented with less ancient, but similarly vast LIPS, the emplacement of the Matachewan LIP likely had a significant impact on the early Proterozoic global environment. Compilation of the best age estimates for individual suites show that the emplacement of the Matachewan LIP occurred synchronously with the Great Oxidation Event. We explore the potential for the eruption of this LIP and the emission of its associated volcanic gases to have been a driver of the irreversible oxygenation of the Earth.

INTRODUCTION

Large Igneous Provinces (LIPs) consist of large volumes (>1.3 × 10^6 km^3) of predominantly mafic-ultramafic magma emplaced during short (1-5 Myr) periods of activity over a maximum lifespan of ~50 Myr (Bryan & Ernst, 2008). LIPs are preserved throughout the geologic record (e.g., Kerr *et al.,* 2000; Ernst & Buchan, 2001) and their study has been used to both understand large-scale mantle processes and also constrain pre-Phanerozoic palaeocontinental reconstructions (e.g., Ernst & Buchan, 2004; Coffin & Eldholm, 2005; Bryan & Ferrari, 2013; Ernst *et al.*, 2013; Ernst, 2014). Currently, the majority opinion favours a mantle plume model for the emplacement of most LIPs, and is even described as 'endemic' by Jones *et al.* (2002). However, other processes for LIP formation have also been proposed, including mantle delamination (Anderson, 2000; McHone, 2000; Anderson, 2005; Elkins-Tanton, 2005; 2007), edge-driven convection (King & Anderson, 1995; 1998; King & Ritsema, 2000; King, 2007), bolide impact (Jones *et al.,* 2002; Ingle & Coffin, 2004; Jones, 2005) and mantle insulation (Anderson, 1982; Doblas *et al.,* 2002; Coltice *et al.,* 2007; 2009).

Coffin & Eldholm (1994) subdivide individual LIPs into three parts: the extrusive zone, the middle crust zone and the lower crustal body. The extrusive zone is dominated by basaltic flows, with occasional felsic members and is associated with the early and late stages of LIP formation. The flow packages can be extremely large, extending laterally for thousands of kilometres and can be tens of kilometres thick (Ernst, 2007; Kerr & Mahoney, 2007). Typically, erosion has removed much of the extrusive zone in older continental LIPs,

though remnants are occasionally preserved within intracratonic basin successions (e.g., Sandeman & Ryan, 2008). The middle crust zone contains the 'plumbing system' of the extrusive zone in the form of dykes, sills and layered intrusions. These plumbing systems are only directly observed in LIPs that are sufficiently old to have had the extrusive cover eroded or to have been dissected by later tectonic events. The most easily recognised features of these plumbing systems are the dykes which form linear dyke sets or massive radiating swarms (Ernst & Buchan, 2001; 2004). The lower crustal body of LIPs is rarely exposed, but is inferred from P-wave velocities of 7.0-7.6 km s^{-1} at the base of the crust beneath more recent LIPs which suggests the presence of an ultramafic underplated layer beneath these systems (Coffin & Eldholm, 2005).

Mafic-ultramafic magmatism occurred on the Superior, Karelia, Kola, Hearne and Wyoming cratons **(Fig. 1)** during the early Proterozoic (~2.45-2.48 Ga). When these cratons are reconstructed as part of the supercraton, 'Superia', the individual igneous suites of the magmatic event comprise a coherent LIP, known as the Matachewan (Bleeker, 2003; Bleeker & Ernst, 2006; Ernst & Bleeker, 2010). This reconstructed Matachewan LIP includes radiating dyke swarms, suites of layered intrusions, sill complexes and flood basalts (Heaman, 1997; Dahl *et al.,* 2006; Van Boening & Nabelek, 2008; Söderlund *et al.,* 2010), which themselves appear to have been emplaced in a series of pulses **(Table 1)**. The layered intrusions are of particular interest because of their economic potential for Ni-Cu-platinum group element (PGE) sulphide mineralisation (Peck *et al.*, 2001; James *et al.,* 2002; Iljina & Hanski, 2005).

Prior to this study, many of the individual igneous suites which make up the Matachewan LIP were poorly-known in terms of their geochemistry and no attempt had been made to study the entire Matachewan LIP utilizing data from all the component blocks, though some attempts have been made to understand the petrogenesis of several individual suites [e.g., Jolly *et al.,* 1992; Phinney & Halls, 2001; Van Boening & Nabelek, 2008; Ciborowski *et al.,* 2013]. In this study we have analysed new samples and compiled existing geochemical data for the reconstructed Matachewan LIP in order to understand the nature and origin of the mantle sources, the anatomy of the magmatic plumbing system within the lithosphere, and how the emplacement of the LIP may have affected the global environment during the Archean-Proterozoic transition.

OVERVIEW OF THE MATACHEWAN LIP

The Matachewan LIP is a proposed ~2.48-2.45 Ga reconstructed LIP found on five separate Archean cratonic blocks (Superior, Wyoming, Hearne, Karelia and Zimbabwe) that comprised the supercontinent 'Superia' (Heaman, 1997; Bleeker & Ernst, 2006; Ernst & Bleeker, 2010; Söderlund *et al.*, 2010) **(Fig. 2)**. Tentative correlations involving rocks associated with the Matachewan LIP have been proposed for decades (Blackwelder, 1926; Young, 1988; Patterson & Heaman, 1991; Williams *et al.*, 1991). However, Roscoe & Card (1993) and Aspler & Chiarenzelli (1998) produced the first detailed sedimentary stratigraphy of, and correlation between, the Superior craton and the Wyoming craton. They suggested that these rocks were either deposited in a common, rift-related intracratonic basin during the break-up of an Archean-Early Proterozoic supercontinent (Kenorland) (Roscoe & Card, 1993) or that the sequences formed as part of a contemporaneous rifted passive margin sequence deposited along the southern margin of the Kenorland supercontinent (Aspler & Chiarenzelli, 1998).

Coeval U-Pb ages (~2.47 Ga) led Heaman (1997) to extend this initial reconstruction to include the Karelia craton following the discovery of radiating dyke swarms on the Superior and Karelia cratons, thus implying a cogenetic source for magmatism on the two cratons. Heaman (1997) was also the first to suggest that a mantle plume was responsible for the break-up of the supercontinent Kenorland and the associated magmatism **(Fig. 2)**.

A comparison of the intrusion history and geochemistry of coeval layered intrusions on the Superior and Karelia cratons (Vogel *et al.*, 1998a), found that the igneous history of the two cratons remained similar until ~2.20 Ga, following which coeval intrusions do not occur on both cratons. A comparison of the dyke swarms in the Superior and Karelian cratons indicated similarity until 2100 Ma (Bleeker & Ernst, 2006) suggesting that breakup did not occur until after, or in association with, the 2025-2100 Ma Marathon LIP and 2075 Ma Fort Frances LIP of the Superior craton and corresponding magmatism on Karelia and the other blocks.

Further, geochemical data for the ~2.48 Ga East Bull Lake layered intrusions (Superior craton) and Fennoscandian intrusions (Karelia craton) suggest that these two suites of intrusions were derived from a common mantle source (Vogel *et al.,* 1998a). The potential ~2.5 Ga link between the Superior, Wyoming and Karelia cratons was further strengthened by Ojakangas *et al.* (2001) who correlated glaciogenic deposits, a palaeosol horizon and carbonate sequences with high $\delta^{13}C$ values between the different cratons.

Using the 'Craton Clan' method, Bleeker (2003) grouped the ~35 Archean cratons into 3-4 craton clans which existed during the Archean – Early Proterozoic. It was proposed that

these clans existed as individual continents separated by intervening oceans, with each continent experiencing a common geologic history prior to continental rifting and tectonic dispersal. One such clan, (the 'Superia' clan) is made up of the Superior, Hearne and Karelia cratons. Using geochronology, petrology and earlier palaeomagnetic work, Bleeker (2004) proposed that these cratons were sutured together prior to 2.45 Ga and that the arrival of a mantle plume head at the end of the Archean initiated magmatism on (and rifting of) the 'Superia' supercontinent. Harlan (2005) proposed that the Leopard Dykes (so called for their ubiquitous plagioclase megacrysts) of the Wyoming craton may be cogenetic with the similarly textured Matachewan and Kaminak dyke swarms on the Superior and Hearne cratons, respectively. However, unpublished U-Pb data indicate that the Leopard dykes were not coeval with the other potential Matachewan LIP suites (K. Chamberlain, *pers. com.,* 2014) and will not be considered here.

A U-Pb date of 2480±6 Ma (Dahl *et al.*, 2006) for the Blue Draw Metagabbro, a 1 km thick layered mafic sill exposed in the eastern Wyoming craton (Ciborowski *et al.*, 2013) strengthens a ~2.5 Ga Superior–Wyoming correlation. This age is identical to the similarly-sized mafic intrusions of the East Bull Lake Intrusive Suite on the Superior craton (Krogh *et al.,* 1984) and suggests a ~ 2.5 Ga supercontinent reconstruction which includes the Wyoming, Superior and Karelia cratons.

Bleeker & Ernst (2006) proposed that temporal matching of the magmatic 'barcodes' for different cratons provides the most robust method for reconstructing ancient continents. Bleeker & Ernst (2006) and also Ernst & Bleeker (2010) and Söderlund *et al.* (2010) presented such 'barcodes' for the Superior, Hearne and Karelia cratons and suggested that these cratons were part of the same supercontinent (Superia) during the late-Archean and Paleoproterozoic until 'Superia' rifted apart sometime after 2.1 Ga.

The most recent ~2.5-2.45 Ga supercontinent reconstruction (Ernst & Bleeker, 2010) links volcano-sedimentary sequences, layered intrusions and mafic dyke swarms on the Wyoming, Superior, Karelia and Hearne cratons and interprets these rocks to have formed during rifting of this supercontinent between ~2.5 and ~2.1 Ga. Crucially, the reconstruction reassembles the mafic dyke swarms preserved on the four constituent cratons into one, giant radiating swarm, thought to indicate the focal point a mantle-plume which drove the rifting event **(Fig. 2)**.

MATACHEWAN LIP SUITES

Matachewan LIP dyke swarms

Matachewan dyke swarm

The Matachewan dyke swarm comprises thousands of north-northwest trending dykes which crop out over an area of 300,000 km^2 in southern Ontario and south western Quebec **(Fig. 1)**. The dykes are sub-vertical and can be up to ~60 m wide, though the majority are ~10-20 m wide (Bates & Halls, 1990; Nelson *et al.,* 1990; Heaman, 1997; Siddorn, 1999). Individual Matachewan dykes can be followed in outcrop over tens of kilometres (Phinney & Halls, 2001), and high resolution aeromagnetic data (West & Ernst, 1991) allows single dykes to be traced in the subsurface for hundreds of kilometres, revealing that they transcend tectonic boundaries between the east-west trending Archean granite-greenstone and metasedimentary terranes which make up the Superior craton. These Fe-rich quartz tholeiite dykes locally contain distinctive plagioclase megacrysts which can be up to ~20 cm in length (Halls, 1991; Siddorn, 1999). Metamorphism of the Matachewan dyke swarm reached a maximum of lower greenschist facies (Halls, 1991).

The Matachewan dyke swarm can be divided into three sub-swarms, characterised by slight changes in dyke orientation and delineated by intervening areas with a low density of dykes (Bates & Halls, 1990; West & Ernst, 1991; Zhang, 1999). Most workers interpret these sub-swarms as being part of a single fanning system with an arc angle of between ~40-60° which radiates from a focus near Sudbury, Ontario (e.g., Ernst *et al.,* 1995; Park *et al.,* 1995; Zhang, 1999; Phinney & Halls, 2001; Halls *et al.,* 2005; Halls *et al.,* 2007). Ages of ~2473 Ma and ~2446 Ma have been obtained for the central and western subswarms, respectively (Heaman, 1997). Halls *et al.* (2005) also dated a Matachewan dyke from west of Kapuskasing (U-Pb baddeleyite) that gave a discordant age of 2459 ± 5 Ma which falls within the range determined by Heaman (1997).

Kaminak dyke swarm

The Kaminak dyke swarm is made up of hundreds of north-northeast trending dykes which crop out over an area of 20,000 km^2 in southern Nunavut (Buchan & Ernst, 2004), approximately 100 km west of Hudson Bay **(Fig. 1)**. The dykes are Fe-rich quartz tholeiites (Christie *et al.*, 1975; Sandeman & Ryan, 2008), range in texture from aphyric to plagioclase porphyritic and locally, can contain abundant megacrysts (~10 cm wide) of plagioclase (Bleeker, 2004). The metamorphism of the bulk of the Kaminak dyke swarm reached a maximum of lower greenschist facies.

The Kaminak dykes are generally vertical and vary from ~1-40 m in thickness, but are typically 5-10 m thick. The dykes tend to form resistant ridges which can be traced over tens of kilometres before being truncated by younger faults (Christie *et al.,* 1975; Sandeman & Ryan, 2008; Sandeman *et al.,* 2013). The N-NE trend of the dykes bisects the dominant tectonic boundaries between the Archean supracrustal and granitoid rocks which make up the hosting Ennadai-Rankin greenstone belt (Aspler *et al.,* 2000). The trends of the Kaminak dykes have been described as radiating, with an arc angle of ~40° by Ernst & Bleeker (2010) or as a linear array (Sandeman & Ryan, 2008). Age data suggests that the Kaminak swarm consists of two pulses of tholeiitic dykes, at 2450 ± 2 Ma and 2498 ± 1 Ma (Heaman, 2004; Sandeman & Ryan, 2008; Sandemann *et al.*, 2013). The older age is more consistent with a link with the 2500 Ma Mistassini LIP of the southeastern Superior craton rather than with the Matachewan LIP (Ernst & Bleeker, 2010). However, the younger age can be linked to the Matachewan LIP.

Based on field relationships and geochemical similarities, the Kaminak dyke swarms have been interpreted to be feeders to the continental tholeiitic basalts of the Spi Group which crop out in the core of a syncline, preserved in the modern day Spi basin (Patterson, 1991; Sandeman & Ryan, 2008).

Viianki dyke swarm

Mafic dyke swarms preserved on the Karelia craton **(Fig. 1)** are poorly defined. Preliminary analysis of the ages of these Paleoproterozoic mafic dykes (Kulikov *et al.,* 2010; see also Vuollo & Huhma, 2005) indicates that the craton experienced at least 3-4 mafic igneous events between 2.4-2.5 Ga which broadly overlap the ages of mafic dykes preserved on the other Superia cratons. Unlike the events on the other cratons, very few attempts have been made to sub-divide the dated Karelia dykes into separate swarms which share a consistent trend, appearance, mineralogy and chemistry.

One of the few Paleoproterozoic swarms to be identified is the Viianki dyke swarm, which has been proposed as the likely feeder of the ~2.44 Ga layered mafic intrusions on the craton (Vogel *et al.,* 1998a). Vogel *et al.* (1998a) characterised the Viianki swarm as a northwest trending swarm of tholeiitic basalt and andesite dykes. The Viianki dykes are likely to be equivalent to the Karelia dykes described by Mertanen *et al.* (1999) based on the similar ages, trends and geographic locations of the dykes. Mertanen *et al.* (1999) describe the Karelia dykes as northwest trending and subvertical, varying in thickness from 6 cm - 200 m

with compositions which range from Fe-tholeiitic and tholeiitic to calc-alkaline. However, these are likely intermixed with c. 1980 Ma dykes and c. 2100 Ma dykes of approximately similar trend (Vuollo & Huhma, 2005).

Matachewan LIP flood basalts

Thessalon Formation

The Huronian Supergroup is a 5-12 km thick volcanic-sedimentary succession which sits unconformably on the Archean basement rocks of the southern Superior Province. The Huronian crops out discontinuously west from the east shore of Lake Superior, through Sudbury to Lake Timiskaming **(Fig. 1)**.

The lowest lithostratigraphic formation in the Huronian Supergroup (Elliot Lake), contains the only ~2.45 Ga volcanic rocks preserved within the supergroup (Krogh *et al.,* 1984; Corfu & Easton, 2000; Ketchum *et al.,* 2013). These volcanic rocks are found in the Thessalon Formation and are preserved in three discrete regions across southern Ontario within which the volcanic rocks range in thickness from 500 – 1200 m (Ketchum *et al.,* 2013).

The Thessalon Formation volcanic rocks are predominantly composed of fine-medium grained basaltic, basaltic-andesitic, andesitic and subordinate rhyolitic flows (Jolly, 1987a; Bennett *et al.,* 1991), which have undergone greenschist facies metamorphism. Bennett *et al.* (1991) reported both ashfall tuffs and pillow basalts within the Thessalon Formation, indicating that eruptions were both subaerial and subaqueous.

Spi Group

The Spi Group is limited to the areally restricted (~8 km^2) Spi Basin in southern Nunavut **(Fig. 1)**, which is interpreted to have formed during the same extension event that resulted in the emplacement of the underlying Kaminak dykes (Sandeman & Ryan, 2008). The lower Spi Group is dominated by the Spi Formation, a 75-150 m thick package of plagioclase porphyritic, basaltic flows with intercalated sediments. The Spi Formation basalts are interpreted to be the eruptive equivalents of the Kaminak dyke swarm (Sandeman *et al.,* 2013). The flows predominantly erupted subareally, though localised, poorly developed pillow structures indicate that at least some were erupted subaqueously.

Based on similar appearances and geochemical signatures, the Spi Formation lavas have been tentatively correlated with other similar plagioclase porphyritic basalts preserved in

other remote basins across southern Nunavut (Carpenter, 2003). This may suggest that the Spi Formation represents the erosional remnants of a much larger flood basalt province, although included fragments have not been found in the unconformably overlying sediments (Sandeman & Ryan, 2008).

Seidorechka Formation

Reconstruction of the Huronian and Karelia Supergroups involve correlations of ~2.45 Ga volcanic rocks that form the base of the Sumi-Sariola Group, here referred to collectively as the Seidorechka Formation (Melezhik, 2006) (see Hanski *et al.* (2001) for a further discussion on the nomenclature and timing of coeval formations). These ~2.45 Ga rocks are preserved in several basins adjacent to the White Sea in northwest Russia and northern Finland **(Fig. 1)**. The Seidorechka Formation is ~3000 m thick and composed of amygdaloidal komatiitic, basaltic and basaltic-andesitic flows at the base and dacitic-rhyolitic flows at the top (Melezhik & Sturt, 1994; Puchtel *et al.,* 1997) that are metamorphosed to lower greenschist facies (Chashchin *et al.,* 2008; Puchtel *et al.,* 1997). Individual flows can be up to ~150 m thick (Puchtel *et al.* 1996) and the original areal extent of the Seidorechka Formation has been estimated to be between 100,000-700,000 km^2 (Melezhik, 2006).

Matachewan LIP layered intrusions

East Bull Lake Suite

The East Bull Lake intrusive suite is the name given to several 2491 – 2475 Ma, layered gabbronoritic to gabbroic-anorthositic intrusions which occur along the margin of the Superior Craton with the Southern Province. The areal extent of individual East Bull Lake Suite intrusions varies from 1 to ~100 km^2. The largest, and most completely preserved of the suite is the 2100 m thick Agnew Lake intrusion, approximately 70 km west of Sudbury, Ontario (Vogel *et al.,* 1998a).

The East Bull Lake Suite intrusions are dominated by leucogabbronoritic and gabbronoritic rocks, though more mafic, melanogabbronorites, troctolites and olivine gabbronorites are found in the lower levels of the intrusions (James *et al.,* 2002). In the most completely preserved East Bull Lake Suite intrusion at Agnew Lake, the stratigraphy at the very top of the intrusion is composed of ferrosyenites and alkali-feldspar granites. Field and geochemical studies of the East Bull Lake suite (Vogel *et al.,* 1998b; 1999) identified the most likely feeder dykes to be the gabbronoritic (An_{78}) Streich dykes. The breccia zones

which are found at the base of many of the East Bull Lake Suite intrusions host contact-style Cu-Ni-PGE mineralisation which has been the focus of continual exploration since the 1980s.

Blue Draw Metagabbro

The 2480 ± 6 Ma Blue Draw Metagabbro is an 800 m thick (~6 km^2 outcrop area) layered amphibolite sill (Dahl *et al.,* 2006) which crops out in the Black Hills uplift, South Dakota, west of Nemo township **(Fig. 1)**. The Black Hills of the Wyoming craton were uplifted during the ~75-35 Ma Laramide Orogeny and expose a complex sequence of basal metaconglomerates and quartzites which are overlain by quartzites, graywackes, iron formations, metavolcanics, gabbros, schists, phyllites and slates which have been deformed during at least three to five separate events (Redden *et al.,* 1990; Hill, 2006). The Blue Draw Metagabbro intrudes the Boxelder Creek Quartzite

Initial work on the Blue Draw Metagabbro by Woo (1952) and Maranate (1979) described the intrusion as a 1 km thick layered sill with serpentinite at the base which grades into hornblendite, plagioclase gabbrodiorite, biotite granodiorite and discontinuous dioritic pegmatite. A series of dominantly NW-SE trending faults have removed the side-wall contacts of the intrusion and have otherwise dismembered the Blue Draw Metagabbro such that slivers of metamorphosed gabbro thought to be correlative with it crop out at several locations throughout the area (Dahl *et al.,* 2006).

Recent work by Ciborowski *et al.* (2013) resampled the Blue Draw Metagabbro and produced a new stratigraphy for the intrusion, that divided it into a 130 m thick peridotite unit which is successively overlain by a ~100 m thick olivine melagabbronorite unit and a ~250 m thick gabbronorite unit. The gabbronorite is overlain by an ~60 m, locally pegamatitic, quartz gabbronorite unit. Unlike its proposed counterparts in the East Bull Lake Suite, no appreciable Ni-Cu-PGE mineralisation has been observed in the Blue Draw Metagabbro.

Fennoscandian Suite

The Fennoscandian suite of layered intrusions is composed of ~20 individual intrusions which crop out in northern Finland and northwest Russia **(Fig. 1)**. These c. 2500-2430 Ma layered intrusions are preserved in two discontinuous belts which transect the Karelia craton (Iljina & Hanski, 2005). The east-west trending Tornio-Näränkävaara Belt crosses Sweden, Finland and Russia between the tip of the Gulf of Bothnia to the White Sea. The second belt trends northwest-southeast across Finland between Kasivarsi and Lake Onega. The rocks are intruded mostly along the contact between Archean tonalitic gneisses and early

Paleoproterozoic volcanic-sedimentary greenstone belts (Alapieti *et al.,* 1990; Weihed *et al.,* 2005). Further north a belt of similar trend occurs along the Kola Peninsula (Kola craton).

These intrusions can be divided into two groups, both spatially and in terms of age, and correlations with different LIPs on the Superior craton (e.g., Kulikov *et al.,* 2010; Ernst & Bleeker, 2010): The older mainly c. 2.50 Ga group of intrusions (including Mt Generalskaya, Monchepluton, Main Ridge and Fedorov-Pansky complex) is restricted to the northernmost belt in the Kola Peninsula, and can be linked to the Mistassini LIP of the eastern Superior craton, Canada. The younger, 'Matachewan-age' c. 2.45 Ga suite of layered intrusions is mainly restricted to the two belts crossing Karelia and can be correlated with the Matachewan magmatism of the Superior craton.

Summary

Although the most widely accepted mechanism for the formation of the Matachewan Large Igneous Province is the impingement of a mantle plume beneath an Archean supercontinent, this is not universally accepted. Volcanic arcs, failed rifts and normal continental and ocean spreading have all been suggested to have formed different component igneous packages of the proposed Matachewan LIP [e.g., Jolly (1987); Van Boening & Nabelek (2008)].

Thus far, geochronology has been key to the development of the Matachewan LIP model, with the most precise ages resulting from U-Pb analyses of baddeleyite. The ages recorded define a period of mafic magmatism which ranges in age between ~2498-2441 Ma that has been interpreted as being pulsatory in nature (Ernst & Bleeker 2010).

GEOCHEMISTRY

This study represents the first attempt to collate representative geochemical data for all of the constituent suites of the Matachewan LIP. These data comes from a mixture of sources including both published and unpublished work, as well as new data collected during this study. The data sources for the Matachewan LIP suites are summarised in **Table 2**. The following sections describe the analytical methods used to collect the new data, how all of the data were screened for alteration and how each of the suites was classified.

Analytical procedures

Sample preparation and analysis for the new geochemical data presented in this paper were carried out at Cardiff University. Weathered surfaces and veins were removed with a rock saw prior to analysis. The samples were then crushed into ~5 mm chips using a steel jaw crusher and powdered in an agate planetary ball mill. Approximately 2 g of the milled powder was ignited in a furnace at 900 °C for two hours in order to determine loss on ignition values.

Whole-rock major element, trace element and rare earth element (REE) data were obtained following Li metaborate fusion (see Minifie *et al.,* 2013). Major element and Sc abundances were determined using a JY Horiba Ultima 2 Inductively Coupled Plasma Optical Emission Spectrometer (ICP-OES). Trace elements were analysed using a Thermo X Series 2 Inductively Coupled Plasma Mass Spectrometer (ICP-MS). International reference material JB-1A was run with each sample batch to constrain the accuracy and precision of the analyses. Relative standard deviations show precision of 1–5% for most major and trace elements for JB-1A. 2σ values encompass certified values for the vast majority of elements. A summary of the whole-rock major element and trace element data for the each of the Matachewan LIP suites is presented in **Table 3**. Full analytical results including repeat runs of standard basalt JB-1A can be found in Supplmentary Data **Electronic Appendix 1**.

To augment the published radiogenic isotope data for the Matachewan LIP **(**Supplmentary Data **Electronic Appendix 2)**, we analysed 18 samples for Sm-Nd and Lu-Hf isotopes from the Blue Draw Metagabbro and East Bull Lake Suite layered intrusions. This work was carried out at the NERC Isotope Geosciences Laboratory in Keyworth, UK. 150-200 mg of sample was weighed into 15ml Savillex Teflon beakers. Mixed ^{149}Sm-^{150}Nd and ^{176}Lu-^{177}Hf isotope tracers were added to the samples prior to dissolution using HF-HNO_3. Primary columns consisting of 2 ml of Eichrom AG50x8 cation exchange resin in 10ml Biorad Poly-Prep columns were used to separate bulk high field strength elements (HFSE: Ti, Hf, Zr), an aliquot containing Sr, Ca and Rb, and a bulk rare-earth element (REE) fraction. Sm, Nd and Lu were separated from the bulk REE fraction using columns consisting of 2 ml of LN-SPEC ion exchange resin, again in Biorad Poly-Prep columns. Hafnium separation followed a procedure adapted from Münker *et al.* (2001) using EICHROM LN-SPEC ion exchange resin in Biorad Poly-Prep columns.

Lu fractions were dissolved in 1 ml of 2% HNO_3 prior to analysis on a Thermo-Electron Neptune mass spectrometer, using a Cetac Aridus II desolvating nebuliser. Hf fractions were dissolved in 1 ml of 2% HNO_3 + 0.1M HF, prior to analysis with a Thermo-Electron Neptune mass spectrometer, using A Cetac Aridus II desolvating nebuliser. Replicate analysis of the BCR-2 rock standard across the time of analysis gave a

mean Lu concentration of 0.49 ppm ± 0.0001 ppm (1-sigma, n=21) while replicate analysis of the JMC475 rock standard across the time of analysis gave a mean Hf concentration of 14.63 ppm ± 0.32 ppm (1-sigma, n=21) and $^{176}Hf/^{177}Hf$ of 0.282150 ± 0.000005.

Sm and Nd fractions were loaded onto one side of an outgassed double Re filament assembly using dilute HCl, and analysed in a Thermo Scientific Triton mass spectrometer. Replicate analysis of the BCR-2 rock standard across the time of analysis gave a mean Sm concentration of 6.34 ± 0.06 ppm (1-sigma, n=7), while replicate analyses of the La Jolla standard across the time of analysis standard gave a $^{143}Nd/^{144}Nd$ of 0.511845 ± 0.000007 (10.4 ppm, 1-sigma).

Element mobility

As many of the Matachewan LIP suites have experienced at least greenschist facies metamorphism (Nelson, 1990; Sandeman & Ryan, 2008), and samples typically show considerable alteration, the effects of secondary element remobilisation must be considered. At metamorphic conditions above lower amphibolite facies the normally immobile high field strength elements (HFSE) including the REE may become more mobile (Pearce, 1996). Therefore, any scatter observed in plots involving these elements for the different Matachewan LIP suite samples may reflect post-solidus changes brought about by their metamorphic history.

To assess if this metamorphism caused secondary element remobilisation of Matachewan LIP lavas, each element was plotted *versus* Zr. Immobile elements that are incompatible in the main rock-forming minerals should fall on correlated, linear arrays when plotted against Zr for a suite of unaltered rocks formed from a common fractionating magma, whereas secondary remobilisation of elements is likely to result in a scattered trend (Cann, 1970).We quantify the strength of the correlations using Pearson's product moment correlation coefficient (R). Elements which have $R^2 \geq 0.75$ are referred to as having a good correlation with Zr; elements with an $0.75 > R^2 \geq 0.5$ are referred to as having a moderate correlation with Zr, and; Elements with an $R^2 < 0.5$ are referred to as having a poor correlation with Zr. Elements whose scatter cannot be explained by a petrogenetic mechanism, or by carrying out statistics on small populations, are inferred to have been remobilised by sub-solidus fluids and are not used to assess petrogenetic processes. A representative subset of these graphs is shown in **(Fig. 3)** and a summary of the R value classes for each element in each suite is given in Supplementary Data **Electronic Appendix 3**.It should be noted that some of the Matachewan LIP suites (e.g., the Matachewan dykes,

and Thessalon Formation) are composite formations made up of two or more geochemically distinct groups which can be defined on the basis of different incompatible trace element ratios (Fig. 4). These are indicated in **Table 3** and R^2 values have been calculated for each distinct group.

Classification

The TAS diagram (LeBas *et al.* 1986) uses K_2O and Na_2O contents to classify igneous rocks. Consequently, the applicability of the TAS diagram for classifying the Matachewan suites (which in certain cases have been metamorphosed to amphibolite facies) is questionable, as these elements have been remobilised in some of the suites. Instead, the Zr/Ti vs. Nb/Y diagram (Pearce, 1996) is potentially more useful as it is based on immobile trace elements. On this diagram the majority of the Matachewan LIP suites plot as overlapping clusters within the subalkaline basalt and basaltic andesite fields. Only the Seidorechka Formation samples plot on a trend of increasing Nb/Y with increasing Zr/Ti between the subalkaline basaltic field and the rhyolite field **(Fig. 5)**.

Geochemical Variation

The most magnesian rocks of the Matachewan LIP belong to the Seidorechka Formation and Viianki dykes, which contain up to 21 wt % MgO. The remaining Matachewan LIP suites contain significantly less MgO (<10 wt %). When plotted on major element bivariate diagrams **(Fig. 6)**, all of the Matachewan suites fall on trends interpreted by Peterson & Moore (1987) to be the result of the initial fractional crystallisation of olivine and subsequent precipitation and removal of plagioclase and clinopyroxene.

All of the Matachewan LIP suites show positive correlations between MgO and elements that are compatible during normal basaltic differentiation such as Cr, Ni, Co and Sc **(Fig. 6)**. Conversely, the incompatible elements (e.g., La, Sm, Yb and Nb) display negative correlations with MgO in all suites. Subtle, yet consistent variations in these trends within individual suites suggest that several of the suites are actually composite formations. These include the Thessalon Formation and Matachewan dykes. Chondrite-normalised REE patterns for the individual Matachewan LIP suites are remarkably similar in that all of the suites show enrichments in the LREE relative to the HREE, that most resemble modern OIB **(Fig. 7)**. In contrast to the majority of Matachewan LIP suites, which have slightly negative Eu anomalies (likely related to fractionation and removal of plagioclase from the primary magma), the Striech dykes have slightly positive anomalies. These anomalies have been interpreted by

Vogel *et al.* (1998b) to be a consequence of megacrystic plagioclase in some of the samples. The parallel nature of the REE patterns of the suites may suggest derivation from a compositionally similar mantle source, albeit via varying degrees of partial melting or fractional crystallisation.

The trace element geochemistry of the Matachewan LIP suites are generally more enriched in the most incompatible elements relative to the least incompatible elements on Primitive Mantle-normalised multi-element diagrams **(Fig. 8)**. All of the suites studied have sizeable negative Nb-Ta and Ti anomalies (where $Nb/Nb^* = Nb_N / [(Th_N + La_N) / 2]$, $Ti/Ti^* = Ti_N / [(Gd_N + Sm_N) / 2]$, where $_N$ denotes primitive mantle normalised value), the largest of which are observed in the Thessalon Formation. Variable anomalies in Zr and Y ($Y/Y^* = Y_N / [(Dy_N + Ho_N) / 2]$) are also observed in some of the Matachewan LIP suites, however, these anomalies are not ubiquitous. For example, variably negative Zr anomalies are observed in six of the eleven suites studied, while in the remaining five suites (including all of the layered intrusion parental magma compositions), no appreciable Zr anomalies are observed. More variable still are the Y anomalies which are found in ten of the Matachewan suites and may be either slightly negative or positive (Y/Y^*[1] range = 0.8-1.1). Their broadly similar trace element geochemistry means that the Matachewan LIP suites consistently plot as overlapping clusters on tectonic discrimination diagrams within fields defined by volcanic-arc basalts, and occasionally (depending on the trace element ratios used) within fields defined by oceanic plateau basalts and mid ocean ridge basalts **(Fig. 9)**.

Isotopic data

Seventeen samples were analysed for Nd-Hf isotopes **(Table 4)**. Six samples were selected from the Blue Draw Metagabbro while four were selected from the East Bull Lake and Agnew intrusions and a further three from the River Valley intrusion. Complimentary whole-rock geochemical data for these samples are available in **Table 5**.

The $\varepsilon Nd_{(i)}$ (where i = 2460 Ma) values of the Blue Draw Metagabbro samples range between -15.4 and -2.3 while the East Bull Lake and River Valley samples range from -3.54 to -0.14 and from -1.00 to -0.57 respectively. Three Agnew samples have a narrow range of $\varepsilon Nd_{(i)}$ values between -0.61 and -1.81 whereas another Agnew sample has an $\varepsilon Nd_{(i)}$ value of -9.78.

The majority of the other Matachewan LIP suites for which isotopic data is available are also characterised by similarly negative εNd_i values (**Fig. 10a**) which have been widely interpreted to be the result of the primary magmas of the province having been derived from an enriched mantle source (e.g., Sandeman and Ryan 2008)) . Only the Matachewan dyke swarm shows significantly positive εNd_i values (up to +3.07) thought to represent the variable contamination of primary magmas derived from partial melting of depleted mantle with Archean crustal material during fractionation in subsurface chambers (Boily and Ludden 1990).

The Blue Draw Metagabbro samples exhibit the largest range in $\varepsilon Hf_{(i)}$ range between -2.3 and +52.6. The East Bull Lake suite intrusions define much smaller ranges such that the East Bull Lake intrusion samples display $\varepsilon Hf_{(i)}$ ranges between -7.6 and +6.3 while the Agnew and River Valley intrusions show even smaller ranges of +3.0 to +5.9 and +2.6 to +5.2 respectively (**Fig. 10b**).

DISCUSSION

Determination of primary magma composition

The relatively evolved nature of the majority of the Matachewan LIP suites (MgO commonly ≤ 9 wt %) suggests that even the most primitive rocks in these suites do not represent primary mantle-derived magmas and have likely evolved through fractionation of olivine ± pyroxene ± plagioclase (as discussed below). To characterise the primary magmas of more evolved suites, Herzberg & Asimow (2008) developed the PRIMELT2 software which can model accumulated perfect fractional melting of mantle peridotite in an attempt to produce viable parent magmas for evolved suites of rocks by computing melt fractions which are capable of; (a) being formed by partial melting of mantle peridotite and (b) replicating the major element composition of the evolved lava through fractionation or accumulation of olivine.

PRIMELT2 is limited in that it is only applicable to peridotite-derived magmas that have been modified by the fractionation or accumulation of olivine. Magmas from pyroxenitic mantle, or those that have undergone fractionation of phases other than olivine, cannot be modelled using PRIMELT2 (Dasgupta *et al.,* 2007; Herzberg & Asimow, 2008).

All of the samples containing > 7.5 wt % MgO (n = 42) from the dyke swarms and flood basalt provinces which make up the Matachewan LIP were assessed using PRIMELT2, as were parental magmas for the layered intrusions. The results are discussed below. For all

samples studied, $Fe^{2+}/\Sigma Fe$ and Fe_2O_3/TiO_2 ratios in the mantle peridotite were kept at 0.9 and 0.5 respectively. **Table 6** shows the major element compositions, degrees of partial melting (F) and potential temperatures (T_P) of all of the primary magmas calculated by PRIMELT2 for each of the Matachewan LIP suites.

PRIMELT2 results

The compositions of magmas parental to the Matachewan LIP layered intrusions have been derived from the compositions of fine-grained, cogenetic dyke feeders (Vogel *et al.,* 1998b; 1999; James *et al.,* 2002), or from calculations of the average composition of the whole intrusion (James *et al.,* 2002; Ciborowski *et al.,* 2013).

PRIMELT2 was able to calculate primary magma compositions for the East Bull Lake Suite parent magmas [sample 234 of Vogel *et al.* (1998a)]. The calculated primary melt contains 18.7 wt % MgO, which is in equilibrium with olivine of composition $Fo_{92.4}$. The degree of partial melting required to produce this primary magma from a peridotite of a composition similar to KR-4003 is 30.3%.

However, PRIMELT2 was unsuccessful in obtaining primary magmas for any of the Thessalon Formation volcanic rocks reported in the literature (Jolly, 1987a; Jolly, 1987b; Jolly *et al.,* 1992; Tomlinson, 1996; Ketchum *et al.*, 2013) or the Seidorechka Formation rocks studied by Chashchin *et al.* (2008). However, PRIMELT2 successfully calculated a primary magma composition for the Seidorechka Formation lavas (sample 91113; Puchtel *et al.,* 1996). This calculated primary magma contains 17.0 wt % MgO, is in equilibrium with olivine of composition $Fo_{91.5}$ and requires 31.1% melting of a mantle peridotite similar in composition to KR-4003.

PRIMELT2 was even less successful in calculating primary magmas for the Kaminak or Matachewan dykes analysed in this study or from the literature (Nelson *et al.,* 1990; Phinney & Hall, 2001; Halls *et al.,* 2005; Ernst & Buchan, 2010) and yielded no feasible primary magma. Though disappointing, the low success rate of PRIMELT2 is not surprising given that the majority of the Matachewan LIP lavas contain < 9 wt % MgO and plot on geochemical variation trends indicative of clinopyroxene and plagioclase fractionation (e.g., Sandeman & Ryan, 2008; Phinney & Halls, 2001). The relatively evolved nature of the Matachewan LIP lavas is likely a product of their intracontinental emplacement setting where, due to limited buoyancy differentials, the primary magmas likely stalled in the lower continental crust (Glazner, 1994; Rudnick & Fountain, 1995) where they fractionated to form

more evolved magmas capable of migrating to higher crustal levels during emplacement of the Matachewan LIP suites studied.

Involvement of a Thermal Plume?

Several lines of evidence have been used to argue for a mantle plume source for the constituent suites of the Matachewan LIP. These include: 1) the radiating patterns of the dyke swarms, resulting from the stresses induced by a plume beneath the lithosphere (Fahrig, 1987; Halls, 1991; Ernst & Buchan, 2001; Phinney & Halls, 2001; Buchan & Ernst, 2004; Ernst & Bleeker, 2010); 2) the coeval nature and sheer volume of magmatism spread across the 'Superia' cratons (Heaman, 1997; Vogel *et al.,* 1998a; Dahl *et al.,* 2006); 3) the high MgO content of some of the suites (Puchtel, 1997); and 4) significant amounts of crustal uplift prior to magmatism (Amelin *et al.,* 1995).

Present day and geologically recent mantle plumes are characterised by upper mantle several hundreds of degrees hotter than ambient mantle (e.g., Wolfe *et al.,* 1997; Bijwaard & Spakman, 1999; Li *et al.,* 2000; Cao *et al.,* 2011). The existence of anomalously high temperature magmatism, indicative of a mantle plume can be investigated by examining the geochemistry of the primary magmas and calculating mantle potential temperature (T_p) - the temperature the mantle would reach if it was brought to the surface adiabatically without melting (McKenzie & Bickle, 1988).

Mantle potential temperatures have been calculated using PRIMELT2 for two of the Matachewan LIP suites; the East Bull Lake Suite and the Seidorechka Formation. The primary magma of the East Bull Lake suite has a calculated T_p of 1545°C, while the primary magma of the Seidorechka Formation (as calculated from the analysis of Puchtel *et al.* (1996)) records a T_p of 1496°C. The total uncertainty in T_P calculated by PRIMELT2 is ± 60°C (2σ) (Herzberg & Asimow, 2008; Herzberg *et al.,* 2010). By comparing these potential temperatures with temperature estimates of the ambient upper mantle at ~2.48-2.45 Ga, we can determine whether the Matachewan LIP magmatism was derived from an anomalously hot upper mantle (i.e., plume) as predicted by mantle plume theory (Campbell, 2007), and confirmed by observations of active mantle plumes (Bijwaard & Spakman, 1999; Li *et al.,* 2000; Montelli *et al.,* 2004; Waite *et al.,* 2006).

Secular cooling models of the mantle suggest that the Paleoproterozoic mantle was significantly hotter than it is today, though by exactly how much is a point of contention. Richter (1988) proposed two cooling models where the starting temperature of the upper

mantle at 4.5 Ga was either 2500°C or 2000°C and cooling proceeded at a continuously decreasing rate to reach a present day value of 1350°C. Regardless of the two starting temperatures used by Richter (1988), his models predict that at ~2.48-2.45 Ga the upper mantle was at ~1500°C. Abbot *et al.* (1994) proposed a cooling history of the upper mantle using fifteen, 3750 Ma samples thought to record N-MORB compositions and calculated the most primitive liquidus temperature for each studied suite. Their model suggests that the upper mantle cooled from ~1700°C at 4 Ga to ~1450°C today. In more recent study, Korenaga (2008) presented a model in which the upper mantle is characterised by an initial increase in temperature from ~1650°C at 4.5 Ga to ~1700°C at 3.6 Ga. This initial increase is followed by an increasingly rapid drop, cooling to a present day value of 1350°C. Subsequent work by Davies (2009) favoured a model of constantly decreasing temperature from an initial upper mantle temperature of 1800°C at 4.5 Ga to reach a modern day temperature of 1300°C. In contrast, Herzberg *et al.* (2010) proposed a model similar to that of Korenaga (2008) whereby an initial warming of the mantle (facilitated by 'sluggish' convection) during the Hadean and Archean led to a mantle temperature maximum at 2.5 – 3.0 Ga that was followed by a continual cooling to reach a modern day temperature of ~1350°C.

The secular cooling models described above are shown in **Fig. 11**. The T_P of the two samples which yield primary magma estimates with PRIMELT2 are also plotted. Seidorechka Formation sample 91113 of Puchtel *et al.* (1996) records a T_p of 1496°C, which is very close to the temperature of the upper mantle at 2.46 Ga predicted by Richter (1988), but ~120°C hotter than the prediction of Davies (2009). The highest T_p sample is the East Bull Lake Suite feeder dyke [sample 234 of Vogel *et al.* (1998a)] which has a calculated T_p of 1545°C. This T_p is 161-57°C higher than the temperature of the upper mantle as modelled by Davies (2009) and Richter (1988) respectively, but lower than that modelled by Korenaga (2008), Herzberg *et al.* (2010) and Abbot *et al.* (1994).

The two most recent cooling models from Davies (2009) and Herzberg *et al.* (2010) – the latter being very similar to that published by Korenaga (2008) – differ hugely (~350°C) in their estimates of T_P during the early Proterozoic. The disparity in these two models stems from the different model parameters used. Davies (2009) argued that some of the assumptions made by Korenaga (2008) regarding plate thickness, Urey ratio (mantle heat production divided by heat loss) and plate curvature at subduction zones appear to be incorrect (Davies, 2009; Karato, 2010). In contrast, Herzberg *et al.* (2010) contend that the high Urey ratio

employed in the model of Davies (2009) is in conflict with cosmochemical constraints on the amount of radiogenic elements in the mantle.

Determining which of the cooling models presented in Figure 11 is more correct is beyond the scope of this work. Indeed, we argue that until more work is carried out to constrain factors such as Urey ratio, effective lithosphere viscosity, secular changes in plate thickness and the radius of curvature for plate bending (upon which such cooling models depend), questions regarding the manner of Earth's secular cooling remain open (Lenardic *et al.,* 2011; Herzberg *et al.*, 2010; Karato, 2010; Davies, 2009).

Fractional Crystallisation

Although, fractional crystallisation can be modelled using the most primitive sample from each suite (i.e., highest MgO and lowest incompatible element concentration), the most primitive sample is unlikely to be a primary magma given the evolved nature of many of the Matachewan LIP suites **(Fig. 6)**. However, the most primitive sample is assumed to be the closest estimate of the primary magma for the suite.

The major element geochemical trends for each of the dyke swarms and flood basalt provinces has been modelled using the PELE computer program (Boudreau, 1999) under five different scenarios **(Table 7)**: *Model 1*: fractional crystallisation at 1 kbar (anhydrous); *Model 2*: fractional crystallisation at 1 kbar (1% H_2O); *Model 3*: fractional crystallisation at 3 kbar (anhydrous); *Model 4*: fractional crystallisation at 7 kbar (anhydrous) and *Model 5*: fractional crystallisation at 10 kbar (anhydrous). All models use a quartz-fayalite- magnetite (QFM) oxygen buffer and calculate the composition of the liquid at 10% crystallisation intervals. The model which best predicts the major element geochemical trends observed in each of the dyke swarms and flood basalt suites is further tested by fractional crystallisation modelling of incompatible trace elements using the mineral assemblages predicted by PELE during crystallisation and the empirically derived mineral/melt partition coefficients given in Supplementary Data **Electronic Appendix 4**.

Where fractional crystallisation fails to accurately model the incompatible element geochemical trends observed in the different Matachewan LIP suites, AFC modelling has been attempted. This modelling uses the mineral assemblages predicted by PELE to form during crystallisation and the empirically derived mineral/melt partition coefficients in Supplementary Data **Electronic Appendix 4**, the composition of felsic crust (Rudnick & Fountain 1995), and the ratio of assimilation/crystallisation which is taken to be 0.3. **Table 8** summarises the results of this petrogenetic modelling.

The majority of the models consistently show that the geochemical trends observed in the Matachewan LIP suites are indicative of AFC processes involving a felsic crustal contaminant **(Fig. 12)**. FC models do not predict the presence of, or changes in, the magnitude of the Nb-Ta and Ti anomalies observed in the majority of the Matachewan LIP suites (Ciborowski *et al.,* 2014). Increasing normalised LREE/HREE ratios are predicted by both the FC and AFC models, though the rate of increase is greater for AFC models and also fits the Matachewan LIP data more convincingly.

In contrast, the trace element geochemistry of the numerous Matachewan Group 1 dykes is best modelled by simple fractional crystallisation with little contamination of the fractionating magmas. However, the significantly negative but variable Ti and Nb anomalies in the Group 1 Matachewan dykes are not predicted by the FC model and may be the product of *in situ* crustal contamination of individual dykes possibly after, or in the later stages of, emplacement.

Mantle Source Composition

Despite the significant amount of field and other evidence that argues for a mantle plume origin for the Matachewan LIP, the geochemical signatures recorded by the constituent suites are more commonly associated with magmas formed in subduction zone settings (Pearce & Peate, 1995). Indeed, these signatures, characterised by significant enrichments in the LREE and LILE, significant negative Nb–Ta and Ti anomalies, and variable Eu anomalies, have been used to argue against a mantle plume mechanism for the petrogenesis of some of the Matachewan LIP suites (e.g., Van Boening & Nabelek, 2008; Jolly, 1987).

In other Paleoproterozoic suites that record field evidence that precludes their having formed in a volcanic arc environment, alternative proposed mechanisms (other than a fundamentally different asthenospheric mantle source) for their arc-like geochemistry include either partial melting of subduction-modified sub-continental lithospheric mantle (SCLM) (Sandeman & Ryan, 2008; Neumann *et al.,* 2011), or, the contamination of mantle melts by continental crust during fractionation in deep crustal magma chambers (e.g., Nelson *et al.,* 1990; Neumann *et al.,* 2011; Jowitt & Ernst, 2013). Below, we attempt to determine whether the action of one of these two mechanisms (mixing of partial melts of the lithospheric mantle vs. crustal contamination) on primary magmas derived from a known mantle reservoir can explain the trace element compositions of the Matachewan LIP suites. This question can be investigated by again looking at the PRIMELT2 data and the degrees of partial melting and fractional crystallisation required to produce the primary magmas of the suites. By applying

these parameters to mantle reservoirs of known composition, potential mantle sources for the Matachewan LIP magmatism may be identified.

Three mantle reservoirs are modelled **(Table 9)**: Depleted MORB Mantle (DMM), Enriched Mantle (EM) and Primitive Mantle (PM). The composition of DMM has been constrained by Workman & Hart (2005) from the trace element depletion trends of abyssal peridotites. The composition of the EM1 reservoir is estimated from inverse modelling of the compositions of EM1 ocean island basalts (Willbold & Stracke, 2006). The composition of PM is derived from studies of chondritic meteorites and refractory element ratios of mantle peridotites (McDonough & Sun, 1995). It should be noted that projecting the existence of these reservoirs, predominantly recognised from modern intraplate basaltic rocks, back into the Palaeoproterozoic is questionable. However, these reservoir compositions can be used to characterise the enriched, depleted or chondritic nature of the Matachewan LIP mantle source region(s).

The ~30% partial melting needed to form the Matachewan LIP primary magmas (as predicted by PRIMELT2) can be modelled using batch melting of spinel lherzolite (Johnson *et al.,* 1990) from the different mantle reservoirs. Spinel lherzolite was chosen for the models as all of the Matachewan LIP suites have relatively flat HREE patterns **(Fig. 7)** which indicates that mantle melting probably occurred within the spinel stability field, or that, if melting occurred deeper, it melted out all of the garnet in the source.

Crustal Contamination

PRIMELT2 predicts that, following partial melting, the Matachewan LIP magmas fractionated variable amounts (7.3–32.3%) of olivine to form the most primitive compositions observed in the suites today. Crustal contamination of these ~30% partial melts of spinel lherzolite can be modelled using the AFC (assimilation fractional crystallisation) equation of DePaolo (1981), the average continental crust composition of Rudnick & Gao (2003) and the degrees of fractionation predicted by PRIMELT2.

Primitive Mantle-normalised multi-element patterns for Seidorechka sample 91113 and East Bull Lake Suite feeder 234, for which PRIMELT2 was able to define partial melting and fractionation parameters, are shown in **Supplementary Data Electronic Appendix 5**. Also plotted are the modelled compositions of magmas formed by AFC of primary magmas derived from melting of spinel lherzolites from the DMM, EM1 and PM mantle reservoirs using the parameters of melting and fractionation listed in **Table 6**. The models consistently show that with larger amounts or higher rates of AFC, primary mantle melts from any of the

reservoirs studied can form magmas which replicate aspects of the trace element geochemistry of the Matachewan suites (negative Nb-Ta and Ti anomalies and LILE-LREE enrichment relative to the HREE). However, for sample 91113, all of the models predict lower La/Sm ratios and much higher HREE contents than those observed in the sample, whereas for the East Bull Lake Suite feeder dyke (sample 234), all of the models predict much greater abundances of HREE than in the sample.

Interaction with SCLM

To determine whether mixing of primary mantle melts with low degree partial melts of subduction-modified SCLM can replicate the trace element composition of the Matachewan LIP suites (as suggested by Sandeman & Ryan, 2008), we have modelled mixing of the primary mantle melts derived from the different mantle reservoirs **(Table 9)** with varying amounts (0.1-5%) of low degree partial melts of subduction-modified SCLM using simple binary mixing. Fractionation of olivine from the resulting mixtures was then modelled to the degree predicted by PRIMELT2.

The estimate for partial melts of the subduction-modified SCLM was taken from an average of 113 analyses of ~1.88 Ga ultrapotassic igneous rocks (minette-lamproite) of the Christopher Island Formation, preserved on the Hearne craton (Sandeman *et al.,* 2003). Despite being significantly younger than the Matachewan LIP magmatism, Sandeman & Ryan (2008) and Cousens *et al.* (2001) argue that the rocks of the Christopher Island Formation represent low degree partial melts of a subcontinental lithospheric mantle source which developed beneath the Hearne and Superior cratons during the Archean and which was, thus, an available source for the Paleoproterozoic Matachewan LIP magmatism. These models show that the mixing of partial melts from the modelled mantle reservoirs with small amounts (~5%) of low degree partial melt from subduction modified SCLM is a viable mechanism for producing the general trace element signatures observed in the Matachewan LIP rocks (LREE enrichment relative to HREE, significant negative Nb-Ta and Ti anomalies). Indeed, the trace element chemistry of Seidorechka Formation sample 91113 (Puchtel *et al.,* 1996), can be closely approximated by a mixture of ~8% SCLM partial melt and 92% DMM partial melt **(Fig. 13)**. In contrast though, the SCLM mixing models produce HREE concentrations that are at least 2-3× higher than those observed in the East Bull Lake Suite feeders **(Supplementary Data Electronic Appendix 6)**.

Two-stage Melting

The two types of model described above attempt to determine whether the trace element signatures observed in the Matachewan LIP suites are better explained by contamination of primary magmas by crustal material during fractionation of the magma in lower crustal bodies, or through mixing of primary magmas with low-degree partial melts of subduction modified SCLM. The models show that the two mechanisms can broadly reproduce the geochemical signatures of the Matachewan LIP samples. This modelling shows that the composition of Seidorechka Formation basalt 91113 can be replicated by a mixture of ~8% SCLM partial melt and 92% DMM partial (F = 0.3) melt. However, for the East Bull Lake Suite feeders, both sets of models over-estimate the abundance of the HREE in the samples studied by a factor of ≥3. Instead, the modelling suggests that in order to produce primary magmas with the HREE contents observed in the East Bull Lake Suite feeder samples (~5.5× chondritic values), partial melting of the DMM spinel lherzolite would need to exceed ~45% which is well in excess of the extent of melting predicted by PRIMELT2.

Thus, if we assume that the modelled mantle reservoirs are applicable to the ~2.48-2.45 Ga Matachewan LIP suites, then the degrees of melting predicted by PRIMELT2 are too low. Alternatively, if we assume that the degrees of partial melting predicted by PRIMELT2 are correct then the trace element compositions of the mantle reservoirs modelled are not representative of the sources of the Matachewan LIP magmatism. The inference is that the Matachewan LIP mantle source was more depleted than any of those modelled.

The existence of a strongly depleted mantle source for the Matachewan LIP magmatism may be inferred by the presence of the ~2.7 Ga greenstone belts (including the Abitibi and Ennadai-Rankin belts of the Superior and Hearne cratons) which host many of the Matachewan LIP suites. These greenstone belts contain large amounts of komatiitic lavas which have been interpreted by Sproule *et al.* (2002) to have formed through ~30% partial melting of the mantle. This partial melting event would have depleted the mantle in incompatible elements such that any further melting events would produce melts with much lower incompatible element contents than the komatiitic lavas of the greenstone belts. If such a residual mantle source persisted beneath the Superia supercontinent (Bleeker, 2003) from its accretion at ~2.7 Ga to the period of melting which formed the Matachewan LIP magmas at ~2.48 Ga, it may have been a source for the Matachewan LIP magmatism.

To test whether melting of such a depleted source is a potential mechanism for producing the trace element compositions observed in the Matachewan LIP suites, models similar to those shown in Supplementary Data **Electronic Appendices 5** and **6** were constructed, this time using the trace element composition of residues of DMM, EM1 and

PM spinel lherzolite formed through 30% batch partial melting as suggested by Sproule *et al.* (2002) and Maier *et al.* (2003). The compositions of these residues are shown in **Table 9**.

AFC models **(Fig. 14)** based on ~30% partial melts of these previously-melted mantle sources in the same way as those in Supplementary Data **Electronic Appendix 5** show that such a mechanism is capable of producing the trace element geochemistry of the Matachewan LIP suites for a previously-melted DMM source which was contaminated by continental crust with an assimilation/fractionation ratio of ~0.4-0.5. Sample 234 is less likely to have been derived from a previously melted EM1 or PM source as it has a $(La/Sm)_N$ ratio higher than those predicted by the model for these reservoirs.

Models which mix partial melts of Archean SCLM with partial melts of previously-melted sources **(Fig. 15)** in the same way as those shown in Supplmentary Data **Electronic Appendix 6** also show that this mechanism is capable of producing the trace element geochemistry of the Matachewan LIP suites using several, but not all of the starting reservoirs. The trace element geochemistry recorded by the East Bull Lake Suite feeder dyke is not compatible with derivation from a previously-melted DMM source, as mixing of partial melts from this source with low degree partial melts of Archean SCLM does not yield mixtures with the observed HREE contents or La/Yb ratios. Alternatively, East Bull Lake Suite feeder dyke 234 may have been derived by mixing of melts of a previously-melted Enriched- or Primitive- Mantle source with low degree partial melts of Archean SCLM in the ratio of ~19:1.

Isotopic considerations

Due to the effects of secondary remobilisation **(Fig. 3)**, Rb-Sr isotopic data cannot be used with confidence when assessing the petrogenesis of the Matachewan LIP. Instead, the Nd-Sm and Lu-Hf systems, which are less susceptible to alteration (Gaffney *et al.,* 2011) are used in the remainder of this study.

Previously published Nd isotopic data for the majority of the Matachewan LIP suites record negative εNd_i values, indicating derivation from enriched mantle sources. New Nd isotopic data for the East Bull Lake suite also records significantly negative εNd_i values, similar in magnitude to the other Matachewan LIP suites, and may be evidence of the intrusions having been derived from similarly enriched primary magmas, or contaminated by continental crust. In terms of the latter, equivalent data for the Blue Draw Metagabbro have the widest range of εNd_i in the Matachewan LIP suites ($-15.09 > \varepsilon Nd_i < -2.46$), the most extremely negative of which have been shown be a feature of the primary magma which

formed the intrusion, and unrelated to *in situ* AFC processes (Ciborowski *et al.,* 2013). This is evidenced by the fact that the earliest formed, and most primitive cumulates have the most extreme εNd_i values, while those rocks with trace element compositions consistent with *in situ* contamination by host-rock material are also the samples with the most positive εNd_i values.

Unfortunately the only Lu-Hf data available for the province is that analysed during this study. Our data show that the majority of the East Bull Lake suite samples have positive εHf_i values of ~+4.0 which suggests that the intrusions were derived from a depleted mantle source. Again, the Blue Draw Metagabbro samples have the most extreme isotopic values ($\varepsilon Hf_i < 53$). Such extreme values are rare in the published literature; however, they have been reported in peridotite mantle xenoliths from the island of O'ahu, Hawai'i. These xenoliths have been interpreted to be derived from ancient (>2 Ga) depleted mantle lithosphere caught up in the upwelling Hawaiian plume (Bizimis *et al.*, 2007).

Invoking a similar reservoir for the Blue Draw Metagabbro is, however, problematic since the O'ahu xenoliths are also characterised by significantly positive εNd values **(Fig. 16)** in contrast to the negative εNd in the Blue Draw Metagabbro samples. Instead, the Blue Draw Metagabbro (and potentially the East Bull Lake suite) were likely derived from a mantle reservoir not recognised in the modern mantle. This reservoir was characterised by high $^{176}Hf/^{177}Hf$ and low $^{143}Nd/^{144}Nd$ ratios relative to the Bulk Earth at 2.46 Ga that cannot be adequately modelled by mixing depleted mantle, similar in composition to the O'ahu xenoliths, with more enriched crustal material.

While seemingly rare in the mantle, extremely positive εHf values (with concomitant negative εNd values) have been observed in kimberlite-hosted Archean-Proterozoic mafic granulites from the Kaapvaal craton (e.g., Schmitz *et al.,* 2004). In these rocks, the apparent decoupling of the Lu-Hf and Sm-Nd isotope systems is argued to be a result of partial melting in the presence of titanomagnetite and ilmenite, but absence of rutile, which itself acts to buffer against Hf depletion in the residue. Assimilation of such material by the primary magmas of the intrusion, prior to its *in situ* fractionation within the Boxelder Creek Quartzite, may explain the extreme εHf values recorded by the Blue Draw Metagabbro. This mechanism, may also help explain the arc-like trace element compositions of the Blue Draw Metagabbro and other related Matachewan LIP suites. To date, however, no such potential contaminants have been documented within the Black Hills uplift which hosts the Blue Draw Metagabbro.

Schmitz *et al.* (2004) also document rutile-bearing felsic granulites that are characterised by –εHf and +εNd values which lie well away from the 'normal' lithosphere array (Vervoort *et al.,* 2000). Schmitz *et al.* (2004) argues that the decoupling of the two isotope systems in these rocks is due to refractory rutile retaining Hf (but not Lu) during low–*P*, high–*T* anatexis, creating a residue characterised by subchondritic Lu/Hf and –εHf values and an isotopically complementary liquid fraction. Mixing of such a liquid with the Blue Draw Metagabbro primary magmas may be a more feasible mechanism than partial melting of mafic granulites for producing the isotopic variation observed in the most primitive samples of the intrusion.

Another possible explanation for the isotopic compositions observed in the Blue Draw Metagabbro comes from Nebel *et al.* (2013, 2014) who report significantly positive εHf_i values in Archean komatiites from the Yilgarn craton which they interpreted to be inherited during partial melting of an ancient, melt-depleted mantle reservoir. Nebel *et al.* (2013, 2014) suggest that such a reservoir – which they term the Early Refractory Reservoir (ERR) – would have formed as the residue left over during the formation of the earliest Hadean terrestrial crust that would have been remelted by hot, upwelling mantle plumes to ultimately produce mafic lavas characterised by superchondritic initial $^{176}Hf/^{177}Hf$ signatures.

Summary

Trace element modelling has shown that both AFC and magma mixing are potential mechanisms for producing the trace element composition of the Matachewan LIP suites. Although trace element modelling is unable to determine which of these processes 'fit' the data better, it suggests that the mantle source for at least the East Bull Lake Suite had been significantly melted prior to its involvement in the formation of the intrusions, potentially during the formation of the 2.8-2.6 Ga greenstone belts which host much of the Matachewan LIP. Alternatively, evidence of this prior melting event may be present in the form of the 2.5 Ga Mistassini LIP, most obviously characterised by the Mistassini radiating dyke swarm preserved on the Superior Craton in Quebec (Ernst & Buchan, 2001). In contrast, the Seidorechka Formation magmatism does not require derivation from such a previously melted source region.

As debate regarding the precise timing of the initiation of plate tectonics and subduction continues (e.g., Harrison *et al.,* 2005; Stern, 2005), the use of reservoirs recognised in the modern mantle which are thought to be related to subduction and recycling

[e.g., Willbold & Stracke (2006)] is questionable. Instead, previous workers have suggested that rather than being the product of contamination or mantle mixing, that the trace element chemistry of the Matachewan LIP, which is ubiquitous in Paleoproterozoic continental magmatic rocks (e.g., Buchan *et al.,* 2007) is due to a fundamental difference in the geochemistry of the ancient mantle compared to the modern mantle.

This explanation was proposed by Vogel *et al.* (1998b) who, when studying the Agnew intrusion of the East Bull Lake suite, noted that the arc-like trace element geochemistry of the East Bull Lake suite feeder dykes is shared by all magmatic rocks coeval with the intrusions on the Superior Craton. Further, global analysis of greenstone belt volcanic rocks and mafic dyke swarms (Condie, 1994; Ernst & Bleeker, 2010) shows that this signature is ubiquitous in such rocks older than ~2 Ga. Vogel *et al.* (1998b) suggest that the ubiquity of this signature in mafic continental intrusions in the Archean-Paleoproterozoic is due to a fundamental difference in the composition of the ancient mantle compared to the modern. Vogel *et al.* (1998b) speculate that this arc-like signature may have been caused by the slow, upward migration of LILE- and LREE-enriched fluids through the mantle during early differentiation of the Earth. They argue that such a process would have metasomatised the entire mantle so that any subsequent partial melts would have a subduction-like geochemical signature. Vogel *et al.* (1998b) argue that continued continental growth, subduction (and recycling) of slabs and partial melting could have obliterated this ephemeral signature by the end of the Paleoproterozoic. The existence of such a mantle reservoir may be recorded by the Nd-Sm and Lu-Hf isotope systematics of the Blue Draw Metagabbro, which are unlike any of the components recognised in the modern mantle.

Potentially more feasible mechanisms for explaining the Nd-Sm and Lu-Hf isotope systematics of the Blue Draw Metagabbro (and perhaps other Matachewan LIP suites), than the cryptic global metasomatism advocated by Vogel *et al.* (1998b) involve the incorporation of material from some sort of lithospheric component, either through assimilation of material produced during Low–*P*, high–*T* anatexis of lithospheric material (Schmitz *et al.,* 2004) or through involvement of an 'Early Refractory Reservoir' (Nebel *et al.,* 2014) residual from the partial melting of the mantle during initial terrestrial crust formation in the Hadean.

In conclusion, the trace element geochemical signatures recorded by the Matachewan LIP suites are common to the majority of Archean-Paleoproterozoic intracontinental magmatic rocks. The debate regarding the mantle source of such widespread magmatic rocks, which retain signatures more associated with modern subduction-related rocks, is ongoing (Gallagher & Hawkesworth, 1992; Xie *et al.,* 1993; Baker *et al.,* 1996; Vogel *et al.,* 1998b;

Sandeman & Ryan, 2008) and not something this study aims to resolve. However, the geochemical modelling presented here suggests that crustal contamination of primary magmas during prolonged residence in the continental crust, or, mixing of the primary magmas from known mantle reservoirs with low degree partial melts of subduction-modified SCLM are potential mechanisms for producing the trace element signatures of the Matachewan LIP suites (assuming the mantle reservoir had already been significantly melted). The models do not require the input of an alternate Archean-Paleoproterozoic mantle reservoir, one which was defined by higher LILE and LREE concentrations relative to HFSE and HREE, but nor do the models rule out the input (or existence) of such a reservoir.

Several LIPs preserved throughout the geological record, including the Siberian Traps, Emeishan LIP and Deccan Traps, have been linked to periods of great environmental upheaval (e.g., Keller *et al.,* 2009; Zhou *et al.,* 2002; Campbell *et al.,* 1992). As such, a review of the Matachewan LIP would not be complete without at least exploring such an avenue. To this end, below we present a discussion of the Matachewan LIP and its potential relationship with the Great Oxidation Event (GOE) which is widely cited to be the first sustained appearance of free oxygen in Earth's atmosphere.

The Matachewan LIP – a cause of the Great Oxidation Event?

It has been proposed that the GOE was a fundamental factor in the evolution of complex multicellular life on Earth (Sessions *et al.,* 2009) and is widely interpreted to have occurred relatively abruptly as evidenced by a number of secular changes in the geological record. One such change relates to the widespread preservation of reduced detrital mineral species in surficial deposits in rocks deposited prior to the Archean-Proterozoic transition, but subsequent absence in sediments younger than the transition (Frimmel, 2005; Sverjensky & Lee, 2010). A second, equally well-documented line of evidence for the GOE may be deduced from studies of sulphur isotopes preserved within sedimentary rocks (e.g., Bekker *et al.,* 2004). Such studies consistently define a transition from mass-independent fractionation of isotopes during the Archean to mass-dependent fractionation in rocks younger than this, which has been argued to signify the stabilisation of ozone (and O_2) in the upper atmosphere (Farquhar & Wing, 2003).

Based on these (and other) lines of evidence, the GOE has been dated to approximately 2450 Ma, that is, hundreds of millions of years after the appearance of photosynthetic cyanobacteria (Sessions *et al.,* 2009). To explain the lag between the onset of

photosynthesis and the oxygenation of the atmosphere, a number of mechanisms have been suggested. These include: a partial cessation of ultramafic volcanism towards the end of the Archean eon, leading to reduced nickel supply to the oceans and concomitant methanogenic bacteria stress (Konhauser *et al.,* 2009); widespread continental collision and orogenesis may have increased nutrient supply to the oceans as well as increasing organic carbon burial rates (Campbell & Allen, 2008); episodes of rifting may have increased the size of the early Proterozoic continental shelf seas, thus promoting organic carbon burial (Lenton *et al.,* 2004); the secular loss of H_2 to space (Kasting, 2013) and a change in volcanic gas composition from more reduced compositions during the Archean to more oxidised compositions during the Proterozoic (Kump & Barley, 2007). More recently, it has been proposed that oxygen released by the reduction of SO_2 (as sulphate ions in seawater) derived from early Proterozoic subaerial volcanism may have driven the GOE (Gaillard *et al.,* 2011).

We argue that against the backdrop of the first emergence of the continents from the oceans during the Archean-Proterozoic transition (Flament *et al.,* 2008), the subaerially erupted lavas of the truly massive Matachewan LIP (Sandeman & Ryan, 2008; Ketchum *et al.*. 2013; Melezhik, 2006) would have resulted in considerable changes to the ancient atmosphere and biosphere. Given the sheer scale of the province, and the fact that the U-Pb geochronological data for the flood basalt suites define an average age of eruption **(Fig. 17)** indistinguishable from the best estimates for the GOE, we suggest that the Matachewan LIP warrants further study as a potential driver of the GOE, arguably the most fundamental event in Earth's history.

CONCLUSIONS

The Matachewan LIP is composed of late Archean-early Proterozoic dyke swarms, layered intrusions and flood basalt provinces preserved on the Superior, Karelia, Wyoming and Hearne cratons. The magmatism is bracketed by the emplacement of members of the East Bull Lake Sute at 2491 Ma and the eruption of the Seidorechka Formation at 2437 Ma, with the entire LIP having an average age of 2461 Ma.

1. The basaltic dyke swarms can be reconstructed as part of the Superia supercraton to radiate out from a point south of Sudbury, Ontario. This point may mark the centre of an early Proterozoic mantle plume which initiated the eventual breakup of Superia.

The mantle plume also resulted in the formation of a large volcanic province, the remnants of which are compositionally similar to the dyke swarms and parent magmas of the layered intrusions.

2. The Matachewan LIP suites all have a broadly similar trace element geochemistry, characterised by enrichment in the most incompatible large ion lithophile and light rare earth elements and depletion in the heavy rare earth and other high field strength elements. This shared geochemistry may suggest the existence of a once widespread mantle reservoir not recognised in the modern mantle that imparted a geochemical signature that is shared by the vast majority of early Proterozoic intracontinental igneous rocks.

3. Alternatively, trace element modelling involving the Matachewan LIP suites suggests their trace element signature can be explained by the contamination of mantle-derived magmas, either by subduction modified sub-continental lithospheric mantle or continental crust during their ascent from the mantle.

4. Comparison of the potential temperatures of the Matachewan LIP suites with the estimates of the early Proterozoic upper mantle suggest that at least parts of the province are derived from mantle hotter than 2.45Ga ambient upper asthenosphere. Given the proposed plume origin of the province, this is not unexpected.

5. The flood basalt volcanism and continental breakup associated with the emplacement of the Matachewan LIP would have caused an enormous perturbation in the Earth's atmosphere. The increase in area of continental shelf on which to bury organic carbon, coupled with a potential sulphur-reducing bacterial bloom initiated by loading the atmosphere with volcanogenic SO_2, could have forced the atmosphere onto a path of irreversible oxygenation, known as the Great Oxidation Event.

ACKNOWLEDGEMENTS

A. Oldroyd, L. Woolley and P. Fisher are thanked for their help in preparation and analysis of samples. Constructive reviews by Oliver Kebel and two anonymous reviewers contributed to significant improvement of the original manuscript

FUNDING

This study forms part of a Ph.D. dissertation undertaken by T.J.R.C. at Cardiff University, United Kingdom, funded by the School of Earth and Ocean Sciences.

REFERENCES

Abbott, D., Burgess, L., Longhi, J. and Smith W. H. F., 1994. An empirical thermal history of the Earth's upper mantle. Journal of Geophysical Research, 99, 13835–13850

Alapieti, T. T., 2005. Chapter 1 - Early Palaeoproterozoic (2.5-2.4 Ga) Tornio - Näränkävaara layered intrusion belt and related chrome and platinum-group element mineralization, Northern Finland. In Guide 51a, eds. T. T. Alapieti and A. J. Kärki. Geological Survey of Finland.

Alapieti, T.T., Filèn, B.A., Lahtinen, J.J., Lavrov, M.M., Smol'kin, V.F. and Voitekhovsky, S.N., 1990. Early Proterozoic layered intrusions in the northeastern part of the Fennoscandian Shield. Mineral. Petrol., 42, pp. 1–22.

Amelin, Y. V. and Semenov, V. S., 1996. Nd and Sr isotopic geochemistry of mafic layered intrusions in the eastern Baltic shield: implications for the evolution of Paleoproterozoic continental mafic magmas. Contributions to Mineralogy and Petrology, 124, 255-272.

Amelin, Y. V., Heaman, L. M. and Semenov, V. S., 1995. U-Pb geochronology of layered mafic intrusions in the eastern Baltic Shield: implications for the timing and duration of Paleoproterozoic continental rifting. Precambrian Research, 75, 31-46.

Anbar, A. D., Duan, Y., Lyons, T. W., Arnold, G. L., Kendall, B., Creaser, R. A., Kaufman, A. J., Gordon, G. W., Scott, C., Garvin, J. and Buick, R., 2007. A Whiff of Oxygen Before the Great Oxidation Event? Science, 317, 1903-1906.

Anderson, D. L., 1982. Hotspots, polar wander, Mesozoic convection and the geoid. Nature, 297, 391-393.

Anderson, D. L., 2000. The Thermal State of the Upper Mantle; No Role for Mantle Plumes. Geophysical Research Letters, 27, 3623-3626.

Anderson, D. L., 2005. Large Igneous Provinces, Delamination, and Fertile Mantle. Elements, 1, 271-275.

Asimow, P. D., and Ghiorso, M. S., 1998. Algorithmic modifications extending MELTS to calculate subsolidus phase relations. American Mineralogist, 83, 1127–1132.

Aspler, L. B. and Chiarenzelli, J. R., 1998. Two Neoarchean supercontinents? Evidence from the Paleoproterozoic. Sedimentary Geology, 120, 75-104.

Aspler, L. B., Armitage, A. E., Ryan, J. J., Hauseux, M., Surmacz, S. and Harvey, B. J. A., 2000. Precambrian geology, Victory and Mackenzie lakes, Nunavut, and significance of 'Mackenzie Lake metasediments', Paleoproterozoic Hurwitz Group. In Current Research, 10.

Baker, J. A., Thirlwall, M. F. and Menzies, M. A., 1996. Sr-Nd-Pb isotopic and trace element evidence for crustal contamination of plume-derived flood basalts: Oligocene flood volcanism in western Yemen. Geochimica et Cosmochimica Acta, 60, 2559-2581.

Balashov, Yu., Bayanova, T. & Mitrofanov, F. 1993 . Isotope data on the age and genesis of layered basic-ultrabasic intrusions in the Kola Peninsula and northern Karelia, northeastern Baltic Shield. Precambrian Research 64, 197-205.

Bayanova, T. & Balashov, Yu. 1995. Geochronology of Palaeoproterozoic layered intrusions and volcanites of the Baltic Shield. Norges Geologiske Undersökelse, Special Paper, 7, 75-80.

Bates, M. P. and Halls, H. C., 1990. Regional variation in paleomagnetic polarity of the Matachewan dyke swarm related to the Kapuskasing Structural Zone, Ontario. Canadian Journal of Earth Sciences, 27, 200-211.

Bekker, A., Holland, H. D., Wang, P. L., Rumble, D., Stein, H. J., Hannah, J. L., Coetzee, L. L. and Beukes, N. J., 2004. Dating the rise of atmospheric oxygen. Nature, 427, 117-120.

Bennett, G., Dressler, B. O. and Robertson, J. A., 1991. The Huronian Supergroup and associated intrusive rocks. In: Thurston, P.C., Williams, H.R., Sutcliffe, R.H. and Stott, G.M., Editors,, Geology of OntarioOntario Geological Survey, Special Volume, 549-591.

Bijwaard, H. and Spakman, W., 1999. Tomographic evidence for a narrow whole mantle plume below Iceland. Earth and Planetary Science Letters, 166, 121-126.

Bizimis, M., Griselin, M., Lassiter, J. C., Salters, V. J. M. and Sen, G., 2007. Ancient recycled mantle lithosphere in the Hawaiian plume: Osmium–Hafnium isotopic evidence from peridotite mantle xenoliths. Earth and Planetary Science Letters, 257, 259-273.

Blackwelder, E., 1926. Precambrian geology of the Medicine Bow Mountains. Geological Society of America Bulletin, 37, 617-658.

Bleeker, W., 2003. The late Archean record: a puzzle in ca. 35 pieces. Lithos, 71, 99-134.

Bleeker, W., 2004. Taking the pulse of planet Earth: a proposal for a new multi-disciplinary flagship project in Canadian solid Earth sciences. Geoscience Canada, 31, 179-190.

Bleeker, W. and Ernst, R., 2006. Short-lived mantle generated magmatic events and their dyke swarms: The key unlocking Earth's paleogeographic record back to 2.6 Ga. In Dyke Swarms - Time Markers of Crustal Evolution. Edited by E. Hanski, S. Mertanen, T. Rämö, and J. Vuollo. Taylor, 3-26.

Blichert-Toft, J., Albarède, F., Rosing, M., Frei, R. and Bridgwater, D., 1999. The Nd and Hf isotopic evolution of the mantle through the Archean. results from the Isua supracrustals, West Greenland, and from the Birimian terranes of West Africa. Geochimica et Cosmochimica Acta, 63, 3901-3914.

Boily, M. and Ludden, N.J., 1990. Trace-element and Nd isotopic variations in Early Proterozoic dyke swarms emplaced in the vicinity of the Kapuskasing structural zone: enriched mantle or assimilation and fractional crystallization (AFC) process? Canadian Journal of Earth Sciences, 28, 26-36.

Boudreau, A. E., 1999. PELE-a version of the MELTS software program for the PC platform. Comput. Geosci., 25, 201-203.

Bryan, S. E. and Ernst, R. E., 2008. Revised definition of Large Igneous Provinces (LIPs). Earth-Science Reviews, 86, 175-202

Bryan, S.E., & Ferrari, L. 2013. Large igneous provinces and silicic large igneous provinces: Progress in our understanding over the last 25 years: Geological Society of America Bulletin, 125, 1053–1078.

Buchan, K. L. and Ernst, R. E., 2004. Diabase dyke swarms and related units in Canada and adjacent regions, Canada and Northern USA. Geological Survey of Canada.

Buchan, K. L., Goutier, J., Hamilton, M. A., Ernst, R. E. and Matthews, W. A., 2007. Paleomagnetism, U-Pb geochronology, and geochemistry of Lac Esprit and other dyke swarms, James Bay area, Quebec, and implications for Paleoproterozoic deformation of the Superior Province. Canadian Journal of Earth Sciences, 44, 643-664.

Buiko, A., Levchenkov, O., Turchenko, S. & Drubetskoi, E. 1995. Geology and isotopic dating of the early Proterozoic Sumian-Sariolian Complex in northern Karelia (Paanajärvi-Tsipringa structure). Stratigraphy, Geological Correlation, 3, 16-30.

Campbell, I. H. and Allen, C. M., 2008. Formation of supercontinents linked to increases in atmospheric oxygen. Nature Geoscience, 1, 554-558.

Campbell, I. H., 2007. Testing the plume theory. Chemical Geology, 241, 153-176.

Cann, J. R., 1970. Rb, Sr, Y, Zr and Nb in some ocean floor basaltic rocks. Earth and Planetary Science Letters, 10, 7-11.

Campbell, I. H., Czamanske, G. K., Fedorenko, V. A., Hill, R. I. and Stepanov, V., 2002. Synchronism of the Siberian Traps and the Permian-Triassic Boundary. Science, 258, 1760-1763.

Cao, Q., van der Hilst, R. D., de Hoop, M.V. and Shim, S.-H., 2011. Seismic imaging of transition zone discontinuities suggests hot mantle west of Hawaii. Science, 332, 1068-1071.

Carpenter, R. L., 2003. Relative and absolute timing of supracrustal deposition, tectonothermal activity and gold mineralization, welst Meliadine regio, Rankin Inlet greenstone belt, Nunaut, Canada. London, Ontario: The Universit of Western Ontario.

Chashchin, V., Bayanova, T. and Levkovich, N., 2008. Volcanoplutonic association of the early-stage evolution of the Imandra-Varzuga rift zone, Kola Peninsula, Russia: Geological, petrogeochemical, and isotope-geochronological data. Petrology, 16, 279-298.

Chauvel, C., Hofmann, A. W. and Vidal, P., 1992. HIMU-EM: The French Polynesian connection. Earth and Planetary Science Letters, 110, 99-119.

Christie, K. W., Davidson, A. and Fahrig, W. F., 1975. The Paleomagnetism of Kaminak Dikes - No Evidence of Significant Hudsonian Plate Motion. Canadian Journal of Earth Sciences, 45, 745-767.

Ciborowski, T.J.R., Kerr, A.C., McDonald, I., Ernst, R.E. and Minifie, M.J., 2013. The geochemistry and petrogenesis of the Blue Draw Metagabbro, Lithos, 174, 271-290.

Ciborowski, T.J.R., Kerr, A.C., McDonald, I., Ernst, R.E., Hughes, H.S.R. and Minifie, M.J., 2014. The geochemistry and petrogenesis of the Paleoproterozoic du Chef dyke swarm, Québec, Canada. Precambrian Research. 10.1016/j.precamres.2014.05.008

Claire, M. W., Catling, D. C. and Zahnle, K. J., 2006. Biogeochemical modelling of the rise in atmospheric oxygen. Geobiology, 4, 239-269.

Cloud, P., 1973. Paleoecological Significance of the Banded Iron-Formation. Economic Geology, 68, 1135-1143.

Coffin, M. F. and Eldholm, O., 1994. Large Igneous Provinces: Crustal Structure, Dimensions, and External Consequences. Reviews of Geophysics, 32.

Coffin, M. F. and Eldholm, O., 2005. Large igneous provinces. In: Selley RC, Cocks R, Plimer IR (Eds). Encyclopedia of Geology, 315-323.

Coltice, N., Bertrand, H., Rey, P., Jourdan, F., Phillips, B. R. and Ricard, Y., 2009. Global warming of the mantle beneath continents back to the Archaean. Gondwana Research, 15, 254-266.

Coltice, N., Phillips, B. R., Bertrand, H., Ricard, Y. and Rey, P., 2007. Global warming of the mantle at the origin of flood basalts over supercontinents. Geology, 35, 391-394.

Condie, K. C., 1994. Chapter 3 Greenstones Through Time. In Developments in Precambrian Geology, ed. K. C. Condie, 85-120. Elsevier.

Condie, K. C., 2005. High field strength element ratios in Archean basalts: a window to evolving sources of mantle plumes? Lithos, 79, 491-504.

Corfu, F. and Easton, R.M., 2001. U–Pb evidence for polymetamorphic history of Huronian rocks within the Grenville front tectonic zone east of Sudbury, Ontario, Canada. Chemical Geology, 172, 149-171.

Cousens, B. L., Aspler, L. B., Chiarenzelli, J. R., Donaldson, J. A., Sandeman, H., Peterson, T. D. and LeCheminant, A. N., 2001. Enriched Archean lithospheric mantle beneath western Churchill Province tapped during Paleoproterozoic orogenesis. Geology, 29, 827-830.

Dahl, P. S., Hamilton, M. A., Wooden, J. L., Foland, K. A., Frei, R., McCombs, J. A. and Holm, D. K., 2006. 2480 Ma mafic magmatism in the northern Black Hills, South Dakota: a new link connecting the Wyoming and Superior cratons. Canadian Journal of Earth Sciences, 1579-1600.

Dasgupta, R., Hirschmann, M. M. and Smith, N. D., 2007. Partial Melting Experiments of Peridotite + CO2 at 3 GPa and Genesis of Alkalic Ocean Island Basalts. Journal of Petrology, 48, 2093-2124.

Davies, G. F., 2009. Effect of plate bending on the Urey ratio and the thermal evolution of the mantle. Earth and Planetary Science Letters, 287, 513-518.

DePaolo, D. J., 1981. Trace element and isotopic effects of combined wallrock assimilation and fractional crystallization. Earth and Planetary Science Letters, 53, 189-202.

Doblas, M., Lopez-Ruiz, J., Cebria, J.-M., Youbi, N. and Degroote, E., 2002. Mantle insulation beneath the West African craton during the Precambrian-Cambrian transition. Geology, 30, 839-842.

Easton, R. M., Davidson, A. and Murphy, E. I., 1999. Tansects across the Southern-Grenville Province boundary near Sudbury, Ontario. In Guidebook, 52. Sudbury: Geological Association of Canada.

Easton, R. M., James, R. S. and Jobin-Bevans, L. S., 2010. Geological Guidebook to the Paleoproterozoic East Bull Lake Intrusive Suite Plutons at East Bull Lake, Agnew Lake and River Valley: a field trip for the 11th International Platinum Symposium. In Open File Report, 108. Ontario Geological Survey.

Elkins-Tanton, L. T., 2005. Continental magmatism caused by lithospheric delamination, . in Foulger, G.R., Natland, J.H., Presnall, D.C., and Anderson, D.L., eds., Plates, plumes, and paradigms:, Geological Society of America Special Paper 388, 449-461.

Elkins-Tanton, L. T., 2007. Continental magmatism, volatile recycling, and a heterogeneous mantle caused by lithospheric gravitational instabilities, Journal of Geophysical Research, 112, B03405.

Ernst, R.E., 2014. Large Igneous Provinces. Cambridge University Press, in press.

Ernst, R. E. and Bleeker, W., 2010. Large igneous provinces (LIPs), giant dyke swarms, and mantle plumes: significance for breakup events within Canada and adjacent regions from 2.5 Ga to the Present. Canadian Journal of Earth Sciences, 47, 695-739.

Ernst, R. E. and Buchan, K. L., 2001. The use of mafic dike swarms in identifying and locating mantle plumes. Geological Society of America Special Papers, 352, 247-265.

Ernst, R. E. and Buchan, K. L., 2004. Large Igneous Provinces (LIPs) in Canada and adjacent regions: 3 Ga to Present. Geoscience Canada, 31, 103-126.

Ernst, R. E., 2007. Large igneous provinces in Canada through time and their metallogenic potential. in Goodfellow, W.D., ed., Mineral Deposits of Canada: A Synthesis of Major Deposit-Types, District Metallogeny, the Evolution of Geological Provinces, and Exploration Methods, Geological Association of Canada, Mineral Deposits Division, Special Publication No. 5, 929-937.

Ernst, R. E., Bleeker, W., Hamilton, M. A. and Söderlund, U., 2008. Continental Reconstructions Back To 2.6 Ga Using The Large Igneous Province (LIP) Record, With Implications For Mineral Deposit Targeting And Hydrocarbon Resource Exploration [extended Abstract]. In Palaeogeography: The Spatial Context for Understanding the Earth System, ed. R. L. P. Markwick, M. Huber (conveners). Cambridge U.K.

Ernst, R. E., Head, J. W., Parfitt, E., Grosfils, E. and Wilson, L., 1995. Giant radiating dyke swarms on Earth and Venus. Earth-Science Reviews, 39, 1-58.

Fahrig, W. F. (1987), The tectonic settings of continental mafic dyke swarms: Failed arm and early passive margin, in Mafic Dyke Swarms, Spec. Pap. 34, edited by H. C. Halls and W. F. Fahrig, pp. 331–348, Geol. Assoc. of Can., St. John's

Farquhar, J. and Wing, B. A., 2003. Multiple sulfur isotopes and the evolution of the atmosphere. Earth and Planetary Science Letters, 213, 1-13.

Frimmel, H. E., 2005. Archaean atmospheric evolution: evidence from the Witwatersrand gold fields, South Africa. Earth-Science Reviews, 70, 1-46.

Gaffney, A. M., Borg, L. E., Asmerom, Y., Shearer, C. K. and Burger, P. V., 2011. Disturbance of isotope systematics during experimental shock and thermal metamorphism of a lunar basalt with implications for Martian meteorite chronology. Meteoritics & Planetary Science, 46, 35-52.

Gaillard, F., Scaillet, B. and Arndt, N. T., 2011. Atmospheric oxygenation caused by a change in volcanic degassing pressure. Nature, 478, 229-232.

Galer, S. J. G. and Mezger, K., 1998. Metamorphism, denudation and sea level in the Archean and cooling of the Earth. Precambrian Research, 92, 389-412.

Gallagher, K. and Hawkesworth, C., 1992. Dehydration melting and the generation of continental flood basalts. Nature, 358, 57-59.

Gates, T. M., and Hurley, P. M., 1973. Evaluation of Rb-Sr dating methods applied to the Matachewan, Abitibi, Mackenzi, and Sudbury, dike swarms in Canada. Canadian Journal of Earth Science, 10, 900-919.

Ghiorso, M. S. and Sack, R. O., 1995. Chemical mass transfer in magmatic processes IV. A revised and internally consistent thermodynamic model for the interpolation and extrapolation of liquid-solid equilibria in magmatic systems at elevated temperatures and pressures. Contributions to Mineralogy and Petrology, 119, 197-212.

Halls, H. C., 1991. The Matachewan dyke swarm, Canada: an early Proterozoic magnetic field reversal. Earth and Planetary Science Letters, 105, 279-292.

Halls, H. C., Kumar, A., Srinivasan, R. and Hamilton, M. A., 2007. Paleomagnetism and U–Pb geochronology of easterly trending dykes in the Dharwar craton, India: feldspar clouding, radiating dyke swarms and the position of India at 2.37 Ga. Precambrian Research, 155, 47-68.

Halls, H. C., Stott, G. M. and Davis, D. W., 2005. Paleomagnetism, geochronology and geochemistry of several Proterozoic mafic dike swarms in northwestern Ontario. Ontario Geological Survey, Open File Report 6171, 59.

Hanski, E., Huhma, H., and Vaasjoki, M., 2001. Geochronology of northern Finland: A summary and discussion. In: Radiometric age determinations from Finnish Lapland and their bearing on the timing of Precambrian volcano-sedimentary sequences (eds) M. Vaasjoki, 255-279. Geological Survey of Finland, Special Paper 33.

Harlan, S. S., 2005. The Paleoproterozoic Leopard Dikes of Montana and Wyoming: A Dismembered fragment of the 2.45Ga Hearst-Matachewan giant radiating dike swarm of the Superior Craton? Geological Society of America Abstracts with Programs, 37, p. 50.

Harlan, S. S., Geissman, J. W. and Premo, W. R., 2003. Paleomagnetism and geochronology of an Early Proterozoic quartz diorite in the southern Rind River Range, Wyoming, USA. Tectonophysics, 362, 105-122.

Harrison, T. M., Blichert-Toft, J., Müller, W., Albarede, F., Holden, P. and Mojzsis, S. J., 2005. Heterogeneous Hadean Hafnium: Evidence of Continental Crust at 4.4 to 4.5 Ga. Science, 310, 1947-1950.

Heaman, L. M., 1997. Global mafic magmatism at 2.45 Ga: Remnants of an ancient large igneous province? Geology, 25, 299-302.

Heaman, L. M., 2004. 2.5-2.4 Ga global magmatism: Remnants or supercontinents or products of superplumes. . Geological Society of America, Abstracts with Programs, 36, 255.

Heimlich, R. A. and Manzer , G. H., 1972. Flow differentiation within Leopard rock dikes, Bighorn Mountains, Wyoming. Earth and Planetary Science Letters, 17, 350-356.

Herzberg, C. and Asimow, P. D., 2008. Petrology of some oceanic island basalts: PRIMELT2.XLS software for primary magma calculation. Geochemisty, Geophysics, Geosystems., 9, Q09001.

Herzberg, C., Condie, K. and Korenaga, J., 2010. Thermal history of the Earth and its petrological expression. Earth and Planetary Science Letters, 292, 79-88.

Hill, J. C., 2006. Structural geology and tectonics of the paleoproterozoic rocks of the Mount Rushmore quadrangle, Black Hills, South Dakota. 160. University of Missouri-Columbia.

Huhma, H., Cliff, R.A., Perttunen, V. and Sakko, M., 1990. Sm–Nd and Pb isotopic study of mafic rocks associated with early Proterozoic continental rifting: the Peröpohja schist belt in northern Finland. Contributions to Mineralogy and Petrology, 104, 369-379.

Iljina, M., 1994. The Portimo Layered Igneous Complex. PhD Thesis. Department of Geology, University of Oulu. Pp. 178.

Iljina, M. and Hanski, E., 2005. Chapter 3 Layered mafic intrusions of the Tornio—Näränkävaara belt. In Developments in Precambrian Geology, eds. P. A. N. M. Lehtinen and O. T. Rämö, 101-137. Elsevier.

Ingle, S. and Coffin, M. F., 2004. Impact origin for the greater Ontong Java Plateau? Earth and Planetary Science Letters, 218, 123-134.

Jackson, S. L., 2001. On the structural geology of the Southern Province between Sault Ste. Marie and Espanola, Ontario. Ontario Geological Survey, Open File Report 55.

James, R. S., Easton, R. M., Peck, D. C. and Hrominchuk, J. L., 2002. The East Bull Lake Intrusive Suite: Remnants of a ~2.48 Ga Large Igneous and Metallogenic Province in the Sudbury Area of the Canadian Shield. Economic Geology, 97, 1577-1606.

Johnson, K. T. M., Dick, H. J. B. and Shimizu, N., 1990. Melting in the oceanic upper mantle: an ion microprobe study of diopsides in abyssal peridotites. Journal of Geophysical Research, 95, 2661-2678.

Jolly, W. T., 1987a. Geology and geochemistry of Huronian rhyolites and low-Ti continental tholeiites from the Thessalon region, central Ontario. Canadian Journal of Earth Sciences, 24, 1360-1385.

Jolly, W. T., 1987b. Lithophile elements in Huronian low-Ti continental tholeiites from Canada, and evolution of the Precambrian Mantle. Earth and Planetary Science Letters, 85, 401-415.

Jolly, W. T., Dickin, A. P. and Wu, T.-W., 1992. Geochemical stratigraphy of the Huronian continental volcanics at Thessalon, Ontario: contributions of two-stage crustal fusion. Contributions to Mineralogy and Petrology, 110, 411-428.

Jones, A. P., 2005. Meteorite Impacts as Triggers to Large Igneous Provinces. ELEMENTS, 1, 277-281.

Jones, A. P., Price, G. D., Price, N. J., DeCarli, P. S. and Clegg, R. A., 2002. Impact induced melting and the development of large igneous provinces. Earth and Planetary Science Letters, 202, 551-561.

Jowitt, S. M. and Ernst, R. E., Geochemical assessment of the metallogenic potential of Proterozoic LIPs of Canada. Lithos. 174, 291-307.

Karato, S.-i., 2010. Rheology of the deep upper mantle and its implications for the preservation of the continental roots: A review. Tectonophysics, 481, 82-98.

Kasting, J. F., 2013. What caused the rise of atmospheric O_2? *Chemical Geology* 362:13-25.

Kerr, A.C., White, R.V. & Saunders, A.D. 2000. LIP reading: Recognizing oceanic plateaus in the geological record. Journal of Petrology, 41, 1041-1056.

Keller, G., Sahni, A. and Bajpai, S., 2009. Deccan volcanism, the KT mass extinction and dinosaurs. Journal of Biosciences, 34, 709-728.

Kerr, A. C. and Mahoney, J. J., 2007. Oceanic plateaus: Problematic plumes, potential paradigms. Chemical Geology, 241, 332-353.

Ketchum, K.Y., Heaman, L.M., Bennet, G. and Hughes, D.J., 2013. Age, petrogenesis and tectonic setting of the Thessalon volcanic rocks, Huronian Supergroup, Canada. Precambrian Research, 233, 144-172.

King, S. D. and Anderson, D. L., 1995. An alternative mechanism of flood basalt formation. Earth and Planetary Science Letters, 136, 269-279.

King, S. D. and Ritsema, J., 2000. African Hot Spot Volcanism: Small-Scale Convection in the Upper Mantle Beneath Cratons. Science, 290, 1137-1140.

King, S. D., 2007. Hotspots and edge-driven convection. Geology, 35, 223-226.

Kirschvink, J. L., Gaidos, E. J., Bertani, L. E., Beukes, N. J., Gutzmer, J., Maepa, L. N. and Steinberger, R. E., 2000. Paleoproterozoic snowball earth: extreme climatic and geochemical global change and its biological consequences. Proceedings of the National Academy of Sciences of the United States of America, 97, 1400-1405.

Komiya, T., Maruyama, S., Hirata, T., Yurimoto, H. and Nohda, S., 2004. Geochemistry of the oldest MORB and OIB in the Isua Supracrustal Belt, southern West Greenland: Implications for the composition and temperature of early Archean upper mantle. Island Arc, 13, 47-72.

Konhauser, K. O., Pecoits, E., Lalonde, S. V., Papineau, D., Nisbet, E. G., Barley, M. E., Arndt, N. T., Zahnle, K. and Kamber, B. S., 2009. Oceanic nickel depletion and a methanogen famine before the Great Oxidation Event. Nature, 458, 750-753.

Konhauser, K.O., Lalonde, S.V., Planavsky, N.J., Pecoits, E., Lyons, T.W., Mojzsis, S.J., Rouxel, O.J., Barley, M.E., Rosi`ere, C., Fralick, P.W., Kump, L.R. and Bekker, A., 2011. Aerobic bacterial pyrite oxidation and acid rock drainage during the Great Oxidation Event. Nature, 478, 369-374.

Korenaga, J., 2008. Urey ratio and the structure and evolution of Earth's mantle. Reviews of Geophysics, 46, 1-32.

Krogh, T. E., Davis, D. W. and Corfu, F., 1984. Precise U-Pb zircon and baddelyite ages for the Sudbury area. In The geology and ore deposits of the Sudbury structure., eds. E. G. Pye, A. J. Naldrett and P. E. Giblin, 431-446.

Kulikov, V. S., Bychkova, Y. V., Kulikova, V. V. and Ernst, R., 2010. The Vetreny Poyas (Windy Belt) subprovince of southeastern Fennoscandia: An essential component of the ca. 2.5–2.4 Ga Sumian large igneous provinces. Precambrian Research, 183, 589-601.

Kump, L. R. and Barley, M. E., 2007. Increased subaerial volcanism and the rise of atmospheric oxygen 2.5 billion years ago. Nature, 448, 1033-1036.

Kump, L., Fallick, A., Melezhik, V., Strauss, H. and Lepland, A., 2013. 8.1 The Great Oxidation Event. In Reading the Archive of Earth's Oxygenation, eds. V. A. Melezhik, A. R. Prave, E. J. Hanski, A. E. Fallick, A. Lepland, L. R. Kump and H. Strauss, 1517-1533. Springer Berlin Heidelberg.

Lauri, L. S., Mikkola, P. and Karinen, T., 2012. Early Paleoproterozoic felsic and mafic magmatism in the Karelian province of the Fennoscandian shield. Lithos, 151, 74-82.

Le Bas, M. J., Le Maitre, R. W., Streckeisen, A. and Zanettin, B., 1986. A Chemical Classification of Volcanic Rocks Based on the Total Alkali-Silica Diagram. Journal of Petrology, 27, 745-750.

Lee, K. H., 1996. Structure and geochemistry of the Nemo area Black Hills, South Dakota, United States of America. Lincoln: University of Nebraska.

Lenton, T. M., Schellnhuber, H. J. and Szathmary, E., 2004. Climbing the co-evolution ladder. Nature, 431, 913-913.

Levchenkov, O., Nikolaev, A., Bogomolov, E. & Yakovleva, S. 1994. U-Pb ages of Sumian acid magmatic rocks in northern Karelia. Stratigraphy, Geological Correlation, 2, 3-9.

Li, X., Kind, R., Priestley, K., Sobolev, S. V., Tilmann, F., Yuan, X. and Weber, M., 2000. Mapping the Hawaiian plume conduit with converted seismic waves. Nature, 405, 938-941.

Lobach-Zhuchenko, S. B., N. A. Arestova, V. P. Chekulaev, L. K. Levsky, E. S. Bogomolov, and I. N. Krylov, 1998. Geochemistry and petrology of 2.40-2.45 Ga magmatic rocks in the north-western Belomorian Belt, Fennoscandian Shield, Russia. Precambrian Research, 92, 223-250.

Maier, W. D., Roelofse, F. and Barnes, S.-J., 2003. The Concentration of the Platinum-Group Elements in South African Komatiites: Implications for Mantle Sources, Melting Regime and PGE Fractionation during Crystallization. Journal of Petrology, 44, 1787-1804.

Manninen, T., Pihlaja, P. & Huhma, H. 2001. U-Pb geochronology of the Peurasuvanto area, northern Finland. In: Vaasjoki, M. (ed.) Radiometric Age Determinations from Finnish Lapland and Their Bearing on the Timing of Precambrian Volcano-Sedimentary Sequences. Geological Survey of Finland, Special Paper, 33, 189-200.

Maranate, S., 1979. Petrogenesis of a layered amphibolite sill in the Nemo district, Black Hills, South Dakota. 60. Rapid City: South Dakota School of Mines and Technology.

McDonough, W. F. and Sun, S. S., 1995. The composition of the Earth. Chemical Geology, 120, 223-253.

McHone, J. G., 2000. Non-plume magmatism and rifting during the opening of the central Atlantic Ocean. Tectonophysics, 316, 287-296.

McHone, J. G., Anderson, D. L., Beutel, E. K. and Fialko, Y. A., 2005. Giant dikes, rifts, flood basalts, and plate tectonics: A contention of mantle models. In Plates, plumes, and paradigms, eds. G. R. Foulger, J. H. Natland, D. C. Presnall and D. L. Anderson, 401-420. Geological Society of America.

McKenzie, D. and Bickle, M. J., 1988. The Volume and Composition of Melt Generated by Extension of the Lithosphere. Journal of Petrology, 29, 625-679.

Melezhik, V. A. and Sturt, B. A., 1994. General geology and evolutionary history of the early proterozoic Polmak-Pasvik-Pechenga-Imandra/Varzuga-Ust'Ponoy greenstone belt in the northeastern Baltic Shield. Earth-Science Reviews, 36, 205-241.

Melezhik, V. A., 2006. Multiple causes of Earth's earliest global glaciation. Terra Nova, 18, 130-137.

Mertanen, S., Halls, H. C., Vuollo, J. I., Pesonen, L. J. and Stepanov, V. S., 1999. Paleomagnetism of 2.44 Ga mafic dykes in Russian Karelia, eastern Fennoscandian Shield — implications for continental reconstructions. Precambrian Research, 98, 197-221.

Minifie, M. J., Kerr, A. C., Ernst, R. E., Hastie, A. R., Ciborowski, T. J. C., Desharnais, G. and Milliar, I. L., 2013. The northern and southern sections of the western ca. 1880 Ma Circum-Superior Large Igneous Province, North America: The Pickle Crow dyke connection? Lithos, 174, 217-235.

Mints, M. V., Glaznev, V. N., Konilov, A. N., Kunina, N. M., Nikitichev, A. P., Raevsky, A. B., Sedikh, Y. N., Stupak, V. M. and Fonarev, V. I. 1996. The Early Precambrian of the Northeastern Baltic Shield: Palaeogeodynamics, Crustal Structure and Evolution. Moscow: Nauchny Mir Pub.

Montelli, R., Nolet, G., Dahlen, F. A., Masters, G., Engdahl, E. R., and Hung, S-H., 2004. Finite-Frequency Tomography Reveals a Variety of Plumes in the Mantle. Science, 16, 338-343.

Munker, C., S. Weyer, E. Scherer, and K. Mezger., 2001. Separation of high field strength elements (Nb, Ta, Zr, Hf) and Lu from rock samples for MC-ICPMS measurements, Geochem. Geophys. Geosyst., 2, 10.1029/2001GC000183

Neal, C. R., Coffin, M. F., Arndt, N. T., Duncan, R. A., Eldholm, O., Erba, E., Farnetani, C., Fitton, J. G., Ingle, S. P., Ohkouchi, N., Rampino, M. R., Reichow, M. K., Self, S. and Tatsumi, Y., 2008. Investigating Large Igneous Province Formation and Associated Paleoenvironmental Events: A White Paper for Scientific Drilling. Scientific Drilling.

Nebel, O., Arculus, R. J., Ivanic, T. J. and Nebel-Jacobsen, Y. J., 2013. Lu–Hf isotopic memory of plume–lithosphere interaction in the source of layered mafic intrusions, Windimurra Igneous Complex, Yilgarn Craton, Australia. Earth and Planetary Science Letters, 380, 151-161.

Nebel, O., Campbell, I. A., Sossi, P. A. and Van Kranendonk, M. J., 2014. Hafnium and iron isotopes in early Archean komatiites record a plume-driven convection cycle in the Hadean Earth. Earth and Planetary Science Letters, 397, 111-120.

Nelson, D. O., Morrison, D. A. and Phinney, W. C., 1990. Open-system evolution versus source control in basaltic magmas: Matachewan-Hearst dike swarm, Superior Province, Canada. Canadian Journal of Earth Sciences, 27, 767-783.

Neumann, E.R., Svensen, H., Galerne, C.Y. and Planke, S., 2011. Multistage Evolution of Dolerites in the Karoo Large Igneous Province, Central South Africa. Journal of Petrology, 10.1093.

Ohta, H., Maruyama, S., Takahashi, E., Watanabe, Y. and Kato, Y., 1996. Field occurrence, geochemistry and petrogenesis of the Archean Mid-Oceanic Ridge Basalts (AMORBs) of the Cleaverville area, Pilbara Craton, Western Australia. Lithos, 37, 199-221.

Ojakangas, R. W., Marmo, J. S. and Heiskanen, K. I., 2001. Basin evolution of the Paleoproterozoic Karelian Supergroup of the Fennoscandian (Baltic) Shield. Sedimentary Geology, 141-142, 255-285.

Park, J. K., Buchan, K. L. and Harlan, S. S., 1995. A proposed giant radiating dyke swarm fragmented by the separation of Laurentia and Australia based on paleomagnetism of ca. 780 Ma mafic intrusions in western North America. Earth and Planetary Science Letters, 132, 129-139.

Patterson, J. G. and Heaman, L. M., 1991. New geochronologic limits on the depositional age of the Hurwitz Group, Trans-Hudson hinterland, Canada. Geology, 19, 1137-1140.

Pearce, J. A. and Peate, D. W., 1995. Tectonic implications of the composition of volcanic arc magmas Annual review of Earth and planetary sciences, 23, 251-285.

Pearce, J. A., 1996. A user's guide to basalt discrimination diagrams. In Trace element geochemistry of volcanic rocks: appliction for massive sulphide exploration, ed. D. Wyman, 79-113. Winnipeg: Geological Association of Canada, Mineral Deposits Division.

Peck, D. C., Keays, R. R., James, R. S., Chubb, P. T. and Reeves, S. J., 2001. Controls on the Formation of Contact-Type Platinum-Group Element Mineralization in the East Bull Lake Intrusion. Economic Geology, 96, 559-581.

Peterson, D.W. and Moore, R.B., 1987. Geologic history and evolution of geologic concepts, Island of Hawaii. In: Decker, R.W., Wright, T.L. and Stauffer P.H. (eds.), Volcanism in Hawaii. USGS Prof. Paper 1350, 1, pp. 149-189.

Phinney, W. C. and Halls, H. C., 2001. Petrogenesis of the Early Proterozoic Matachewan dyke swarm, Canada, and implications for magma emplacement and subsequent deformation. Canadian Journal of Earth Sciences, 38, 1541-1563.

Puchtel, I. S., Haase, K. M., Hofmann, A. W., Chauvel, C., Kulikov, V. S., Garbe-Schönberg, C. D. and Nemchin, A. A., 1997. Petrology and geochemistry of crustally contaminated komatiitic basalts from the Vetreny Belt, southeastern Baltic Shield: Evidence for an early Proterozoic mantle plume beneath rifted Archean continental lithosphere. Geochimica et Cosmochimica Acta, 61, 1205-1222.

Puchtel, I. S., Hofmann, A. W., Mezger, K., Shchipansky, A. A., Kulikov, V. S. and Kulikova, V. V., 1996. Petrology of a 2.41 Ga remarkably fresh komatiitic basalt lava lake in Lion Hills, central Vetreny Belt, Baltic Shield. Contributions to Mineralogy and Petrology, 124, 273-290.

Räsänen, J. & Huhma, H., 2001. U-Pb datings in the Sodankylä schist area of the Central Lapland Greenstone Belt. In: Vaasjoki, M. (ed.) Radiometric Age Determinations from Finnish Lapland and Their Bearing on the Timing of Precambrian Volcano-Sedimentary Sequences. Geological Survey of Finland, Special Paper. 33, 153-188.

Redden, J. A., Peterman, Z. E., Zartman, R. E. and DeWitt, E. R., 1990. U-Th-Pb geochronology and preliminary interpretation of Precambrian events in the Black Hills, South Dakota. In The Trans-Hudson orogen. Edited by J.F. Lewry and M.R. Stauffer, Geological Association of Canada Special Paper 37, 229-251.

Richter, F. M., 1988. A Major Change in the Thermal State of the Earth at the Archean-Proterozoic Boundary: Consequences for the Nature and Preservation of Continental Lithosphere. Journal of Petrology, Special_Volume, 39-52.

Roscoe, S. M. and Card, K. D., 1993. The reappearance of the Huronian in Wyoming: rifting and drifting of ancient continents. Canadian Journal of Earth Sciences, 30, 2475-2480.

Rudnick, R. L. and Fountain, D. M., 1995. Nature and composition of the continental crust: a lower crustal perspective. Reviews of Geophysics, 33, 267-309.

Rudnick, R. L. and Gao, S., 2003. 3.01 - Composition of the Continental Crust. In Treatise on Geochemistry, eds. D. H. Editors-in-Chief: Heinrich and K. T. Karl, 1-64. Oxford: Pergamon.

Sandeman, H. A. and Ryan, J. J., 2008. The Spi Lake Formation of the central Hearne domain, western Churchill Province, Canada: an axial intracratonic continental tholeiite trough above the cogenetic Kaminak dyke swarm. Canadian Journal of Earth Sciences, 45, 745-767.

Sandeman, H. A., Cousens, B. L. and Hemmingway, C. J., 2003. Continental tholeiitic mafic rocks of the Paleoproterozoic Hurwitz Group, Central Hearne sub-domain, Nunavut: insight into the evolution of the Hearne sub-continental lithosphere. Canadian Journal of Earth Sciences, 40, 1219-1237.

Sandeman, H. A., Heaman, L. M. and LeCheminant, A.N., 2013. The Paleoproterozoic Kaminak dykes, Hearne craton, western Churchill Province, Nunavut, Canada: Preliminary constraints on their age and petrogenesis. Precambrian Research, 232, 119-139.

Schmitz, M. D., Vervoort, J. D., Bowring, S. A. and Patchett, P. J., 2004. Decoupling of the Lu-Hf and Sm-Nd isotope systems during the evolution of granulitic lower crust beneath southern Africa. Geology, 32, 405-408.

Schopf, J.W., 1993. Microfossils of the Early Archean Apex chert: new evidence of the antiquity of life. Science, 260, 640–646.

Sessions, A. L., Doughty, D. M., Welander, P. V., Summons, R. E. and Newman, D. K., 2009. The Continuing Puzzle of the Great Oxidation Event. Current Biology, 19, R567-R574.

Siddorn, J.P., 1999. Differential uplift of the Archean Basement North of the Sudbury Basun: Petrographic Evidence from the Matachewan Dyke Swarm. 62. University of Toronto.

Söderlund, U., Hofmann, A., Klausen, M. B., Olsson, J. R., Ernst, R. E. and Persson, P.-O., 2010. Towards a complete magmatic barcode for the Zimbabwe craton: Baddeleyite U–Pb dating of regional dolerite dyke swarms and sill complexes. Precambrian Research, 183, 388-398.

Sproule, R. A., Lesher, C. M., Ayer, J. A. and Thurston, P. C., 2003. Geochemistry and metallogenesis of komatiitic rocks in the Abitibi greenstone belt, Ontario. ed. O. G. Survey, 119.

Stern, R.J., 2005. Evidence from ophiolites, blueschists, and ultrahigh-pressure metamorphic terranes that the modern episode of subduction tectonics began in Neoproterozoic time. Geology, 33, 557-560.

Sun, S. s. and McDonough, W. F., 1989. Chemical and isotopic systematics of oceanic basalts: implications for mantle composition and processes. Geological Society, London, Special Publications, 42, 313-345.

Sverjensky, D. A. and Lee, N., 2010. The Great Oxidation Event and Mineral Diversification. ELEMENTS, 6, 31-36.

Tomlinson, K. Y., 1996. The geochemistry and tectonic setting of early Precambrian greenstone belts, Northwestern Ontario, Canada. PhD thesis. pp. 287. University of Portsmouth.

Van Boening, A. M. and Nabelek, P. I., 2008. Petrogenesis and tectonic implications of paleoproterozoic mafic rocks in the Black Hills, South Dakota. Precambrian Research, 167, 363-376.

Vervoort, J. D., Patchett, P. J., Blichert-Toft, J. and Albarède, F., 1999. Relationships between Lu–Hf and Sm–Nd isotopic systems in the global sedimentary system. Earth and Planetary Science Letters, 168, 79-99.

Vogel, D. C., James, R. S. and Keays, R. R., 1998a. The early tectono-magmatic evolution of the Southern Province: implications from the Agnew Intrusion, central Ontario, Canada. Canadian Journal of Earth Sciences, 35, 854-870.

Vogel, D. C., Vuollo, J. I., Alapieti, T. T. and James, R. S., 1998b. Tectonic, stratigraphic, and geochemical comparisons between ca. 2500-2440 Ma mafic igneous events in the Canadian and Fennoscandian Shields. Precambrian Research, 92, 89-116.

Vogel, D. C., Keays, R. R., James, R. S. and Reeves, S. J., 1999. The Geochemistry and Petrogenesis of the Agnew Intrusion, Canada: A Product of S-Undersaturated, High-Al and Low-Ti Tholeiitic Magmas. Journal of Petrology, 40, 423-450.

Vuollo, J. and Huhma, H., 2005. Chapter 5 Paleoproterozoic mafic dikes in NE finland. In Developments in Precambrian Geology, eds. P. A. N. M. Lehtinen and O. T. Rämö, 195-236. Elsevier.

Waite, G. P., Smith, R. B. and Allen, R. M., 2006. VP and VS structure of the Yellowstone hot spot from teleseismic tomography: Evidence for an upper mantle plume. Journal of Geophysical Research, 111, B04303.

Walter, M. J., 1998. Melting of garnet peridotite and the origin of komatiite and depleted lithosphere. Journal of Petrology, 39, 29-60.

Weihed, P., Arndt, N. T., Billström, K., Duchesne, J.-C., Eilu, P., Martinsson, O., Papunen, H. and Lahtinen, R., 2005. 8: Precambrian geodynamics and ore formation: The Fennoscandian Shield. Ore Geology Reviews, 27, 273-322.

West, G. F. and Ernst, R. E., 1991. Evidence from aeromagnetics on the configuration of Matachewan dykes and the tectonic evolution of the Kapuskasing Structural Zone, Ontario, Canada. Canadian Journal of Earth Sciences, 28, 1797-1811.

Willbold, M. and Stracke, A., 2006. Trace element composition of mantle end-members: Implications for recycling of oceanic and upper and lower continental crust. Geochemisty, Geophysics, Geosystems, 7, Q04004.

Williams, H., 1991. Anatomy of North America: thematic geologic portrayals of the continent. Tectonophysics, 187, 117-134.

Wolfe, C. J., Bjarnason, I. T., VanDecar, J. C. and Solomon, S. C., 1997. Seismic structure of the Iceland mantle plume. Nature, 385, 245-247.

Woo, C. C., 1952. The Pre-Cambrian geology and amphibolites of the Nemo district, Black Hills, South Dakota. 148. Chicago: University of Chicago.

Workman, R. K. and Hart, S. R., 2005. Major and trace element composition of the depleted MORB mantle (DMM). Earth and Planetary Science Letters, 231, 53-72.

Xie, Q., Kerrich, R. and Fan, J., 1993. HFSE/REE fractionations recorded in three komatiite-basalt sequences, Archean Abitibi greenstone belt: Implications for multiple plume sources and depths. Geochimica et Cosmochimica Acta, 57, 4111-4118.

Young, G. M., 1988. Proterozoic plate tectonics, glaciation and iron-formations. Sedimentary Geology, 58, 127-144.

Zhang, B., 1999. A Study of Crustal Uplift along the Kapuskasing Zone Using 2.45 Ga Matachewan Dykes. In Department of Geology. Toronto: University of Toronto.

Zhou, M-F., Malpas, J., Song, X-Y., Robinson, P. T., Sun, M., Kennedy, A. K., Lesher, C. M. and Keays, R. R., 2002. A temporal link between the Emeishan large igneous province (SW China) and the end-Guadalupian mass extinction. Earth and Planetary Science Letters, 196, 113-122.

Figure captions

Fig. 1. Maps showing the present day positions of the cratons which make up the reconstructed Archean supercontinent, Superia. Also shown are the locations of the mafic dyke swarms, layered intrusions and volcano-sedimentary rift basins which have been proposed to constitute the reconstructed Matachewan LIP. Volcano-sedimentary rift basins: Snowy Pass Supergroup – SP, Spi Group – SG, Huronian Supergroup – HU, Karelian Supergroup – KS; Layered intrusions: East Bull Lake Suite – EBLS, Blue Draw Metagabbro – BDM, Fennoscandian Intrusions – FI; Mafic dyke swarms: Leopard – LE, Kaminak – KA, Matachewan – MA, Viianki – VI, Streich – ST.

Fig. 2. Early Proterozoic Matachewan LIP reconstruction. The mafic dyke swarms, layered intrusions and volcano-sedimentary rift basins are preserved on the Superior, Wyoming, Hearne, Karelia and Kola cratons. When reconstructed to their inferred primary distribution, the composite radiating dyke swarm defines a mantle plume locus, melting at which triggered the emplacement of the Matachewan LIP. Abbreviations as in Fig. 1. Modified after Söderlund *et al.* (2010).

Fig. 3. Major and trace element variation diagrams *vs* Zr for the Matachewan LIP suites.

Fig. 4. Trace element ratio diagrams for the Matachewan dykes and Thessalon Formation basalts. (a) La/Sm *vs* Gd/Yb; (b) Nb/Th *vs* La/Yb

Fig. 5. Zr/Ti *vs* Nb/Yb classification diagram (after Pearce, 1996) for the Matachewan LIP suites.

Fig. 6. Major and trace element variations *vs* MgO for the Matachewan LIP suites.

Fig. 7. Chondrite-normalised rare earth element patterns for the average composition of each of the Matachewan LIP suites. EMORB, NMORB, OIB values are from Sun & McDonough (1989). Chondrite normalising values from McDonough & Sun (1995).

Fig. 8. Primitive mantle-normalised trace element patterns for the average composition of each of the Matachewan LIP suites. EMORB, NMORB, OIB values from Sun & McDonough (1989). Primitive Mantle normalising values from McDonough & Sun (1995).

Fig. 9. Zr/Nb *vs* Nb/Th (a) and Nb/Y *vs* Zr/Y (b) for the Matachewan LIP suites. Field boundaries and end-member compositions from Condie (2005). Abbreviations: PM = Primitive Mantle, DM = shallow depleted mantle, ARC = arc related basalts, NMORB = normal mid-ocean ridge basalt, OPB = oceanic plateau basalt, OIB = oceanic island basalt, DEP = deep depleted mantle, REC = recycled component.

Fig. 10. εNdi (a), and εHfi (b) variations for the Matachewan LIP suites. Data for East Bull Lake Suite and Blue Draw Metagabbro (BDM) from this study. Sources of data for the other suites are in Table 2. Initial isotope ratios (i) calculated for t = 2460 Ma.

Fig. 11. Thermal evolution of the upper mantle through times using different models; A – Davies (2009); B – Richter (1988); C – Abbot *et al.* (1994); D – Korenaga (2008) and Herzberg *et al.* (2010).

Fig. 12. Crystallisation models used in this study (for the Kaminak dykes). (a) and (b) major element models showing the best fit of Model 4 (7 kbar, anhydrous, QFM) in reproducing the major element variation in the Kaminak dykes. Line markers denote 10% crystallisation intervals of the parent magma. (c) Primitive Mantle-normalised trace element patterns for the Kaminak dykes and range of compositions predicted to form through AFC using the mineral assemblage and degrees of fractionation predicted by Model 4, and the composition of average crust (Rudnick & Fountain 1995) where r = 0.1 and F = fraction of liquid remaining. Normalising values from McDonough & Sun (1995).

Fig. 13. Primitive Mantle-normalised multi-element patterns for 31.1% partial melt of spinel lherzolite from the DMM (a), EM1 (b) and PM (c) mantle reservoirs which have mixed with between 0.1-5% low degree partial melts of Archaean SCLM (Sandeman *et al.,* 2003) before fractionating 7.31% olivine. Also plotted is the analysis of the Seidorechka Formation basalt 91113 (Puchtel *et al.,* 1996). Primitive Mantle normalising values from McDonough & Sun (1995).

Fig. 14. Primitive Mantle-normalised multi-element patterns for 30.3% partial melts of spinel lherzolite from DMM (a), EM1 (b) and PM (c) which have been previously melted (F = 0.3). The compositions have been modified by 7.3% AFC of olivine using the bulk continental

crust (Rudnick & Gao 2003) as the contaminant for r = 0.1-0.5. Also plotted is the analysis of East Bull Lake Suite feeder dyke 234 (Vogel *et al.,* 1998b). Primitive Mantle normalising values from McDonough & Sun (1995).

Fig. 15. Primitive Mantle-normalised multi-element patterns for 30.3% partial melts of spinel lherzolite from the DMM, EM1 and PM reservoirs which have been previously melted (F = 0.3). The compositions have been modified by mixing with 0.1, 1 and 5% low degree partial melts of Archaean SCLM (Cousens *et al*., 2001) before undergoing 32.32% FC of olivine. Also plotted is the analysis of East Bull Lake Suite feeder dyke sample 234 (Vogel *et al.*, 1998b). Primitive Mantle normalising values from McDonough & Sun (1995).

Fig. 16. Variation of εNdt vs. εHft for the Matachewan LIP layered intrusions analysed in this study. For comparison fields for other Archean-Paleoproterozoic components are plotted: ISB = Isua Supracrustal Belt conglomerates, turbidites and gneisses (Blichert-Toft *et al.,* 1999); WIC = Windimurra Igneous Complex gabbros (Nebel *et al.,* 2013); OP = Peridotite mantle xenoliths from O'ahu (Bizimis *et al.,* 2007); ASAG = Archean lower crustal South African granulites (Schmitz *et al.,* 2004). Values calculated for t = 2.46 Ga.

Fig. 17. Variation of $\Delta^{33}S$ versus geological age (modified after Johnson *et al.,* 2011). Note the prevalence of mass-independent fractionation of sulphur isotopes in rocks older than 2450 Ma and subsequent absence in rocks deposited since the early Proterozoic. This change in the geological record is argued to signify the first sustained appearance of oxygen in Earth's atmosphere during the Great Oxidation Event. Also plotted are age estimates for each of the individual Matachewan LIP suites. References: A – Krogh *et al.* (1984), B – Easton *et al.* (1999), C – Lauri *et al.* (2012), D – Dahl *et al.* (2006), E – Heaman (1997), F – Halls *et al.* (2005), G – Heaman (1994), H – Sandeman *et al.* (2013), I – Mertanen *et al.* (1999), J – Ketchum *et al.* (2013), K – Amelin *et al.* (1995), L – Puchtel *et al.* (1997), M – Chashchin *et al.* (2008), N – Anbar *et al.* (2007), O – Schopf (1993).

Table 1. Summary of reported ages for constituent Matachewan LIP suites. Locations in parentheses indicate undated suites that have been interpreted as cogenetic with associated suites (see text for discussion). Abbreviations: bad – baddeleyite, zir – zircon, tit – titanite.

Suite	Age (Ma)	Analysis type	Reference
Mafic Dyke Swarms			
Matachewan	2446 ± 3	bad + zir	Heaman (1997)
	2473 $^{+16}_{-9}$	bad	Heaman (1997)
	2459 ± 5	bad	Halls *et al*. (2005)
Kaminak *(Spi Group)*	2450 ± 2	bad	Heaman (1994)
	2498 ± 1	bad	Sandeman *et al*. (2013)
Viianki	2446 ± 5	bad	Mertanen *et al.* (1999)
Flood Basalt Provinces			
Thessalon Formation	2450 $^{+25}_{-10}$	zir	Krogh *et al.* (1984)
	2453 ± 3	zir	Ketchum *et al*. (2013)
Seidorechka Formation			
Seidorechka	2434 ± 15	bad + zir	Bayanova & Balashov (1995)
Imandra	2442 ± 2	bad	Amelin *et al*. (1995)
Paanajärvi	2432 ± 22	zir	Buiko *et al*. (1995)
Lekhta	2443 ± 5	zir	Levchenkov *et al*. (1994)
Vetreny Belt	2437 ± 3	zir	Puchtel *et al*. (1997)
Sakiamaa	2438 ± 11	zir	Räsänen & Huhma (2001)
Rookkiaapa	2438 ± 14	zir	Manninen *et al.* (2001)
Khibiny	2448 ± 8	zir	Chashchin *et al*. (2008)
Layered Intrusions			
Blue Draw Metagabbro	2480 ± 6	tit	Dahl *et al*. (2006)
East Bull Lake Suite *(Streich dykes)*			
East Bull Lake	2480 $^{+10}_{-5}$	bad + zir	Krogh *et al.* (1984)
Agnew	2491 ± 5	zir	Krogh *et al.* (1984)
River Valley	2476 $^{+2}_{-1}$	bad + zir	Unpub. in Easton *et al.* (1999)
Fennoscandian Intrusions	2424 ± 5 – 2470 ± 9	bad + zir	Comp. in Lauri *et al*. (2012)
	2432 ± 6 – 2496 ± 10	bad + zir	Comp. in Hanski *et al*. (2001)

Table 2. Summary of the nature and sources of data collated during this study for each of the Matachewan LIP suites.

Suite	Analysis type	# analyses	Data Source
Mafic Dyke Swarms			
Matachewan	Majors + Traces	60	This study
Kaminak	Majors + Traces	57	This study
	Sm - Nd	9	Sandeman *et al*. (2013)
Viianki	Majors + Traces	6	Vogel *et al*. (1998a)
	Sm-Nd	5	Mertanen *et al*. (1999)
Streich	Majors + Traces	4	Vogel *et al*. (1998a)
Flood Basalt Provinces			
Thessalon Formation	Majors + Traces	79	Tomlinson (1996); Ketchum *et al*. (2013)
	Sm - Nd	12	Jolly *et al*. (1992)
Seidorechka Formation	Majors + Traces	100	Mints *et al*. (1996); Puchtel *et al*. (1997);
	Sm - Nd	38	Puchtel *et al*. (1997)
Spi Group	Majors + Traces	8	Sandeman & Ryan (2008)
	Sm - Nd	5	Sandeman & Ryan (2008)
Layered Intrusions			
Blue Draw Metagabbro	Majors + Traces	105	This study
	Sm - Nd	6	This study
	Lu - Hf	6	This study
East Bull Lake Suite	Majors + Traces	38	This study
	Sm - Nd	11	This study
	Lu - Hf	11	This study
Fennoscandian Intrusions	Sm - Nd	168	Huhma *et al*. (1990); Balashov *et al*. (1993); Iljina (1994); Amelin & Semenov (1996); Puchtel *et al*. (1997); Lobach-Zhuchenko *et al*. (1998); Hanski *et al*. (2001)

Table 3. Summary of the key geochemical ranges and averages of the Matachewan LIP suites. † - estimate of Blue Draw Metagabbro parent magma from Ciborowski et al. (2013). N denotes normalisation to Primitive Mantle of Sun & McDonough (1989). Sources of data are described in Table 2.

Suite	MgO (wt.%)	Fe_2O_3 (wt.%)	SiO_2 (wt.%)	Alkali (wt.%)	Ni (ppm)	Cr (ppm)	$(La/Sm)_N$	$(Gd/Yb)_N$	Eu/Eu*	Nb/Th	Zr/Nb	Zr/Y	Nb/Y	Nb/Nb*	Ti/Ti*	Zr/Zr*	Y/Y*
Mafic Dyke Swarms																	
Matachewan																	
Group 1	2.2-8.8	11.0-18.0	48.4-55.7	2.3-5.6	8-170	9-476	2.0	1.1	0.9	3.0	19.8	3.6	0.2	0.5	0.8	1.0	1.1
Group 2	23.0-5.9	11.2-14.6	48.3-53.5	4.1-7.1	8-817	5-339	2.8	2.2	0.9	1.5	21.7	6.6	0.3	0.2	0.6	0.9	1.1
Kaminak	2.2-6.3	13.5-17.1	45.4-54.0	3.2-5.4	11-220	4-89	2.9	1.5	1.0	1.5	20.9	4.7	0.2	0.2	0.8	0.9	1.1
Flood Basalts																	
Thessalon Formation																	
Group 1	4.1-7.1	10.1-17.0	45.2-56.6	2.2-8.2	49-152	23-179	2.4	1.5	0.9	1.7	21.1	4.3	0.2	0.3	0.6	0.9	0.9
Group 2	1.5-8.2	10.2-16.7	47.8-61.7	3.3-7.4	1-205	1-44	2.9	2.9	0.9	3.6	14.5	7.7	0.5	0.6	0.5	0.7	0.8
Group 3	8.4-9.9	12.5-14.6	50.1-52.9	2.8-3.9	302-357	997-1080	2.5	2.3	0.9	5.5	10.3	6.2	0.6	0.7	0.5	0.8	0.9
Group 4	3.7-5.2	9.7-13.3	53.1-58.1	3.1-6.5	63-78	27-30	3.6	1.5	0.7	0.7	16.7	5.2	0.3	0.2	0.4	0.8	0.9
Seidorechka Formation	0.5-20.8	4.2-12.3	48.2-76.0	2.8-7.2	0-700	0-1400	3.4	1.6	0.8	-	31.2	6.3	0.2	0.3	0.6	1.2	1.0
Spi Group	2.5-3.5	12.6-13.9	49.3-53.8	3.5-54.9	41-66	28-39	3.1	1.7	0.8	1.4	18.7	5.9	0.3	0.2	0.7	0.9	1.0
Layered Intrusion parent magmas																	
Blue Draw Metagabbro†	13	10.2	52.9	3.9	20-1357	20-3131	3.2	1.5	0.9	0.8	22.8	5.3	0.2	0.1	0.5	1.0	1.0
Fennoscandian Intrusion feeders (Viianki dykes)	8.2-17.2	9.9-11.5	50.7-53.4	1.7-3.8	209-510	520-1708	3.0	1.7	1.0	1.3	37.3	5.4	0.2	0.2	0.6	1.0	0.9
East Bull Lake Suite feeders (Streich dykes)	7.5-8.0	10.0-10.5	49.1-50.4	2.6-3.7	27-709	10-604	2.1	1.1	1.3	2.1	27.1	3.4	1.3	0.3	0.8	1.0	1.0

Table 4. New Sm-Nd and Lu-Hf isotope data for selected Matachewan LIP layered intrusions. εNd_i and εHf_i calculated for 2460 Ma, $(^{147}Sm/^{144}Nd)_{CHUR} = 0.1967$ and $(^{176}Lu/^{177}Hf)_{CHUR} = 0.0332$.

Suite	Sample	Rb	Sr	$^{87}Sr/^{86}Sr$	$^{87}Rb/^{86}Sr$	$(^{87}Sr/^{86}Sr)_i$	Nd	Sm	$^{147}Sm/^{144}Nd$	$^{143}Nd/^{144}Nd$	εNd_i	Lu	Hf	$^{176}Lu/^{177}Lu$	$^{176}Hf/^{177}Hf$	εHf_i
Blue Draw Metagabbro	BD096	6.9	142.1	0.707821	0.0011	0.707781	1.757	0.547	0.1881	0.511947	-10.83	0.107	1.393	0.0109	0.282261	19.09
	BD091	13.9	132.8	0.710585	0.0014	0.710535	3.570	0.935	0.1582	0.511743	-5.31	0.137	1.305	0.0150	0.282154	8.47
	BD078	0.2	134.3	0.712903	0.0008	0.712875	1.149	0.485	0.2550	0.512854	-14.31	0.106	0.994	0.0151	0.282707	27.91
	BD037	0.3	1.3	0.728534	0.0008	0.728506	0.503	0.108	0.1296	0.511394	-3.04	0.024	0.375	0.0089	0.281975	12.18
	BD044	0.2	26.5	0.710054	0.0019	0.709987	0.973	0.410	0.2550	0.512815	-15.09	0.063	0.589	0.0151	0.283396	52.34
	BD065	46.9	217.4	0.716918	0.0004	0.716904	8.787	1.862	0.1280	0.511399	-2.46	0.218	2.570	0.0121	0.281706	-2.64
East Bull Lake	EB002	5.9	655.8	0.704678	0.026017	0.703753	7.238	1.608	0.1342	0.511618	-0.14	0.242	0.963	0.0357	0.282670	-7.73
	EB003	12.2	131.9	0.707692	0.267563	0.698180	2.178	0.714	0.1981	0.512481	-3.53	0.158	0.605	0.0370	0.283127	6.24
	EB005	16.2	363.0	0.707081	0.129090	0.702491	1.521	0.377	0.1497	0.511842	-0.67	0.074	0.445	0.0237	0.282415	3.11
	EB006	14.4	143.2	0.709568	0.290944	0.699225	2.124	0.546	0.1554	0.511863	-2.06	0.123	0.909	0.0192	0.282172	2.06
Agnew	AG003	4.8	279.0	0.704965	0.049754	0.703196	3.591	0.894	0.1505	0.511857	-0.61	0.134	0.992	0.0193	0.282212	3.36
	AG004	35.8	397.2	0.706368	0.260692	0.697101	1.811	0.473	0.1577	0.511913	-1.81	0.118	0.731	0.0230	0.282448	5.58
	AG006	13.8	200.8	0.706171	0.198775	0.699105	4.055	1.067	0.1591	0.511990	-0.74	0.219	0.976	0.0318	0.282791	2.94
	AG007	27.0	259.8	0.710113	0.300703	0.699423	0.759	0.286	0.2274	0.512637	-9.78	0.086	0.354	0.0347	0.282922	2.91
River Valley	RV006	15.0	277.5	0.707949	0.156369	0.702390	3.789	0.925	0.1474	0.511810	-0.57	0.146	0.674	0.0307	0.282732	2.78
	RV009	16.8	763.1	0.706268	0.063676	0.704004	3.425	0.918	0.1620	0.512039	-0.72	0.168	0.554	0.0432	0.283386	5.15
	RV014	20.8	424.2	0.705460	0.141833	0.702048	2.426	0.496	0.1235	0.511400	-1.00	0.113	0.846	0.0190	0.282171	2.41

Table 5. Whole-rock geochemical data for samples of Matachewan LIP layered intrusions analysed by this study for Rb-Sr, Sm-Nd and Lu-Hf isotopes.

	Blue Draw Metagabbro						East Bull Lake Intrusion				Agnew Intrusion				River Valley Intrusion		
	BD037	**BD044**	**BD065**	**BD078**	**BD091**	**BD096**	**EB002**	**EB003**	**EB005**	**EB006**	**AG003**	**AG004**	**AG006**	**AG007**	**RV006**	**RV009**	**RV014**
Majors (wt.%)																	
SiO_2	37.45	50.58	55.06	54.40	52.75	44.91	49.24	48.54	48.50	45.32	50.28	49.18	50.19	50.24	50.63	48.64	53.01
TiO_2	0.12	0.28	0.62	0.25	0.37	0.30	0.38	0.33	0.18	0.25	0.47	0.33	0.38	0.20	0.34	0.60	0.19
Al_2O_3	2.43	3.44	13.89	8.94	8.40	15.19	22.77	11.89	24.44	14.81	24.58	24.21	13.26	15.82	22.44	9.35	17.10
Fe_2O_3	10.84	8.24	10.71	7.89	10.74	7.13	5.93	14.41	4.86	13.37	6.29	6.35	13.65	8.90	4.79	13.89	9.43
MnO	0.13	0.18	0.17	0.15	0.18	0.13	0.09	0.21	0.09	0.21	0.09	0.08	0.18	0.15	0.10	0.17	0.14
MgO	38.94	19.88	6.15	12.06	13.38	7.79	0.65	11.03	4.18	11.62	2.89	3.10	7.40	8.50	3.48	13.67	6.33
CaO	0.10	13.07	9.42	10.06	10.22	10.71	18.26	9.63	12.77	8.23	12.96	11.27	12.25	10.18	12.77	9.89	8.15
Na_2O	0.01	0.99	2.82	0.73	1.64	2.47	1.37	1.35	2.38	1.18	2.36	2.79	1.67	2.35	3.30	1.73	3.40
K_2O	0.00	0.03	1.31	0.22	0.45	0.28	0.19	0.46	0.64	0.31	0.31	1.03	0.31	0.40	0.48	0.71	0.86
P_2O_5	0.01	0.02	0.08	0.01	0.03	0.05	0.06	0.02	0.02	0.03	0.04	0.02	0.04	0.01	0.04	0.15	0.01
LOI	11.18	3.58	0.63	4.41	1.98	10.73	1.08	1.86	1.71	3.61	0.80	1.33	0.75	1.71	1.38	2.04	1.72
Total	101.20	100.29	100.86	99.11	100.14	99.69	100.01	99.74	99.77	98.95	101.08	99.70	100.09	98.47	99.74	100.84	100.35
Traces (ppm)																	
Sc	8.9	45.2	28.7	37.9	34.1	23.5	6.9	37.2	16.9	15.0	17.7	11.7	43.9	24.8	22.4	40.0	17.3
Zr	14.6	20.4	97.7	21.4	47.7	37.6	51.0	22.2	22.0	28.9	38.5	24.7	38.8	12.9	25.5	19.2	30.4
V	43.4	225.9	203.3	208.2	245.8	149.2	151.7	165.7	87.4	106.2	121.5	88.8	189.8	325.6	110.4	226.2	59.1
Cr	3390.9	1567.1	110.3	641.9	628.7	130.3	10.4	257.3	412.1	64.5	103.6	82.6	164.1	187.1	153.1	604.2	139.8
Co	127.3	46.0	39.1	32.2	57.8	31.0	6.1	77.4	22.8	79.8	22.8	26.7	49.7	47.3	23.2	66.4	47.4
Ni	1236.7	365.0	168.5	160.6	199.5	130.8	26.6	275.7	119.7	450.3	68.1	175.6	107.9	253.9	41.3	347.9	708.5
Cu	34.8	37.7	47.0	90.5	39.8	27.8	27.5	82.1	45.8	62.5	47.5	143.2	88.6	57.8	70.0	473.7	2911.8
Ga	3.7	5.3	16.6	10.9	10.3	12.6	26.0	11.9	15.4	11.9	16.6	17.7	15.7	14.8	16.1	14.6	15.8
Rb	0.3	0.2	46.9	0.2	13.9	6.9	5.9	12.2	16.2	14.1	4.8	35.8	13.8	27.0	15.0	16.8	20.8
Sr	1.1	27.3	217.4	145.1	128.6	142.5	649.3	130.5	363.4	146.4	305.8	420.2	214.5	275.9	284.7	742.5	450.6
Y	3.2	7.0	15.7	7.0	10.1	7.2	16.0	9.2	5.0	6.9	9.2	7.9	16.0	5.8	9.2	9.8	6.5
Nb	46.43	10.28	329.60	15.08	205.87	85.63	39.88	167.39	107.80	116.23	70.34	211.98	130.69	231.98	238.48	325.48	269.12
La	2.08	3.27	16.46	3.61	8.16	6.45	14.65	5.59	5.62	5.53	5.19	6.50	7.44	4.21	4.57	4.38	7.45
Ce	3.31	6.17	34.10	7.68	17.77	12.52	19.75	6.00	5.43	8.27	9.47	9.49	12.53	4.94	8.66	7.78	13.53
Pr	0.38	0.82	4.07	0.99	2.22	1.58	2.44	0.81	0.68	1.04	1.23	1.24	1.68	0.80	1.14	1.10	1.57
Nd	1.58	3.50	15.40	4.12	8.33	5.82	9.72	3.65	2.81	4.16	5.06	5.14	7.23	3.18	4.54	4.95	5.78
Sm	0.38	0.89	3.25	0.98	1.98	1.28	2.28	1.06	0.73	1.00	1.23	1.26	1.92	0.81	1.17	1.31	1.11
Eu	0.12	0.27	0.96	0.32	0.59	0.39	1.01	0.45	0.40	0.38	0.50	0.67	0.76	0.44	0.50	0.64	0.67
Gd	0.36	1.02	3.20	0.98	1.90	1.22	2.23	1.05	0.65	0.94	1.24	1.22	2.00	0.73	1.23	1.25	0.91
Tb	0.07	0.17	0.49	0.16	0.30	0.19	0.38	0.19	0.10	0.15	0.21	0.19	0.36	0.12	0.20	0.21	0.16
Dy	0.45	1.16	2.98	1.12	1.99	1.32	2.49	1.38	0.73	1.00	1.40	1.24	2.38	0.81	1.28	1.37	0.95
Ho	0.08	0.23	0.54	0.23	0.38	0.25	0.51	0.29	0.16	0.21	0.28	0.24	0.48	0.17	0.26	0.29	0.20
Er	0.25	0.67	1.63	0.63	1.14	0.75	1.52	0.87	0.45	0.61	0.82	0.70	1.40	0.47	0.80	0.85	0.62
Tm	0.04	0.11	0.27	0.11	0.17	0.11	0.25	0.15	0.07	0.10	0.13	0.11	0.23	0.08	0.13	0.14	0.09
Yb	0.28	0.69	1.69	0.64	1.13	0.74	1.69	1.00	0.48	0.65	0.89	0.77	1.58	0.54	0.92	1.01	0.80
Lu	0.04	0.10	0.25	0.10	0.17	0.11	0.28	0.16	0.07	0.10	0.13	0.12	0.25	0.09	0.12	0.14	0.13
Hf	0.33	0.49	2.53	0.66	1.55	0.94	1.32	0.51	0.50	0.70	1.15	0.65	1.05	0.36	0.58	0.48	0.82
Ta	0.05	0.05	0.37	0.07	0.17	0.15	0.11	0.02	0.03	0.06	0.10	0.07	0.08	0.06	0.07	0.04	0.12
Pb	1.21	0.94	12.98	2.88	5.21	3.32	8.29	2.51	4.86	45.73	5.12	13.34	2.74	6.42	8.99	6.35	6.95
Th	0.72	0.86	5.94	1.06	2.93	2.02	1.56	0.28	0.34	0.67	0.78	0.51	0.92	0.35	0.60	0.23	1.97
U	0.17	0.21	1.71	0.27	0.70	0.47	0.54	0.09	0.12	0.18	0.22	0.18	0.24	0.33	0.14	0.11	0.95

Table 6. Primary magma compositions for different Matachewan LIP suites as calculated by PRIMELT2. T – eruption temperature; T_P – mantle potential temperature; F – degree of melting; Fo – forsterite content of olivine in equilibrium with the melt; % ol – percentage of olivine added to sample composition needed to obtain primary magma composition.

Sample	Suite	SiO_2	TiO_2	Al_2O_3	Cr_2O_3	Fe_2O_3	FeO	MnO	MgO	CaO	Na_2O	K_2O	NiO	P_2O_5	T (°C)	T_P (°C)	F	Fo	% ol
91113	**Seidorechka Formation**	49.03	0.56	10.78	0.22	1.14	9.13	0.18	17.04	9.76	1.78	0.24	0.07	0.08	1390	1508	31.1	91.5	7.3
234	**Streich Dykes**	47.06	0.35	12.82	0.02	0.83	9.04	0.18	18.69	8.94	1.47	0.43	0.16	0.01	1422	1545	30.3	92.4	32.3

Table 7. Model parameters used in PELE for investigation of fractional crystallisation models.

Model	Pressure	H_2O content	Oxygen buffer
Model 1	1 kbar	0%	QFM
Model 2	1 kbar	1%	QFM
Model 3	3 kbar	0%	QFM
Model 4	7 kbar	0%	QFM
Model 5	10 kbar	0%	QFM

Table 8. Summary of the modelling showing the MgO content of the parent magma, most successful model parameters, predicted crystallisation sequence, the degree of fractionation required to account for the geochemical variation observed and the preferred mechanism for each of the Matachewan LIP suites studied. Abbreviations: sp – spinel, ol – olivine, cpx – clinopyroxene, plg – plagioclase, opx – orthopyroxene, or – orthoclase, qz – quartz, FC – fractional crystallisation, AFC – assimilation-fractional crystallisation.

Suite	MgO cont. parent	Pressure (kbar)	1 wt.% H_2O	Liquidus temp. (°C)	Crystallisation sequence	% FC recorded	Preferred mechanism
Matachewan Dykes (Grp. 1)	8.8	7	×	1375	sp, ol, cpx, plg	60	FC
East Bull Lake Suite	6.6-7.7	3	×	1267-1251	sp, plg, ol, cpx, opx, qz, or	100	AFC
Thessalon Formation (Grp. 1)	6.7	1	✓	1245	sp, ol, plg, cpx	30	AFC
Thessalon Formation (Grp. 2)	6.8	10	×	1378	sp, opx, cpx, plg	60	AFC
Blue Draw Metagabbro	13.0	3	×	1446	ol, sp, plg, cpx, opx, or, qz	100	AFC
Kaminak Dykes	6.3	7	×	1283	sp, cpx, plg	60	AFC
Viianki Dykes	8.0	1	✓	1475	sp, ol, cpx	30	AFC
Seidorechka Formation	20.8	1	×	1479	ol, opx, sp, cpx, plg, qz	90	AFC

Element (ppm)	DMM	EM1	PM	C_S DMM F = 0.3	C_S EM1 F = 0.3	C_S PM F = 0.3
Th	0.01	0.03	0.09	0.00008	0.00027	0.00081
Nb	0.15	0.38	0.71	0.00100	0.00260	0.00480
Ta	0.01	0.03	0.04	0.00007	0.00018	0.00028
La	0.19	0.60	0.69	0.00600	0.01800	0.02000
Ce	0.55	1.75	1.78	0.02900	0.09400	0.09500
Pr	0.11	0.29	0.28	0.00900	0.02300	0.02200
Nd	0.58	1.47	1.35	0.06200	0.15700	0.14500
Zr	5.00	13.00	11.00	0.64300	1.58900	1.41800
Hf	0.16	0.36	0.31	0.02200	0.05100	0.04400
Sm	0.24	0.52	0.44	0.05000	0.10700	0.09200
Eu	0.10	0.20	0.17	0.02300	0.04900	0.04100
Ti	716	1433	1300	198	396	360
Gd	0.36	0.72	0.60	0.09300	0.18700	0.15600
Tb	0.07	0.13	0.11	0.01900	0.03700	0.03000
Dy	0.51	0.92	0.74	0.14800	0.27000	0.21600
Y	3.33	5.77	4.55	0.91100	1.58000	1.24600
Ho	0.12	0.20	0.16	0.03700	0.06600	0.05300
Er	0.35	0.60	0.48	0.12200	0.21200	0.16900
Tm	0.05	0.09	0.07	0.02000	0.03400	0.02700
Yb	0.37	0.62	0.49	0.12100	0.20400	0.16300
Lu	0.06	0.10	0.07	0.02000	0.03300	0.02600

Table 9. Trace element compositions of mantle end-members modelled in this study. Data sources: DMM – Workman & Hart (2005), EM1 – Willbold & Stracke (2006), PM – McDonough & Sun (1995). Also shown are the trace element compositions of the mantle end-member residues (C_S) following 30% batch partial melting of spinel lherzolite.

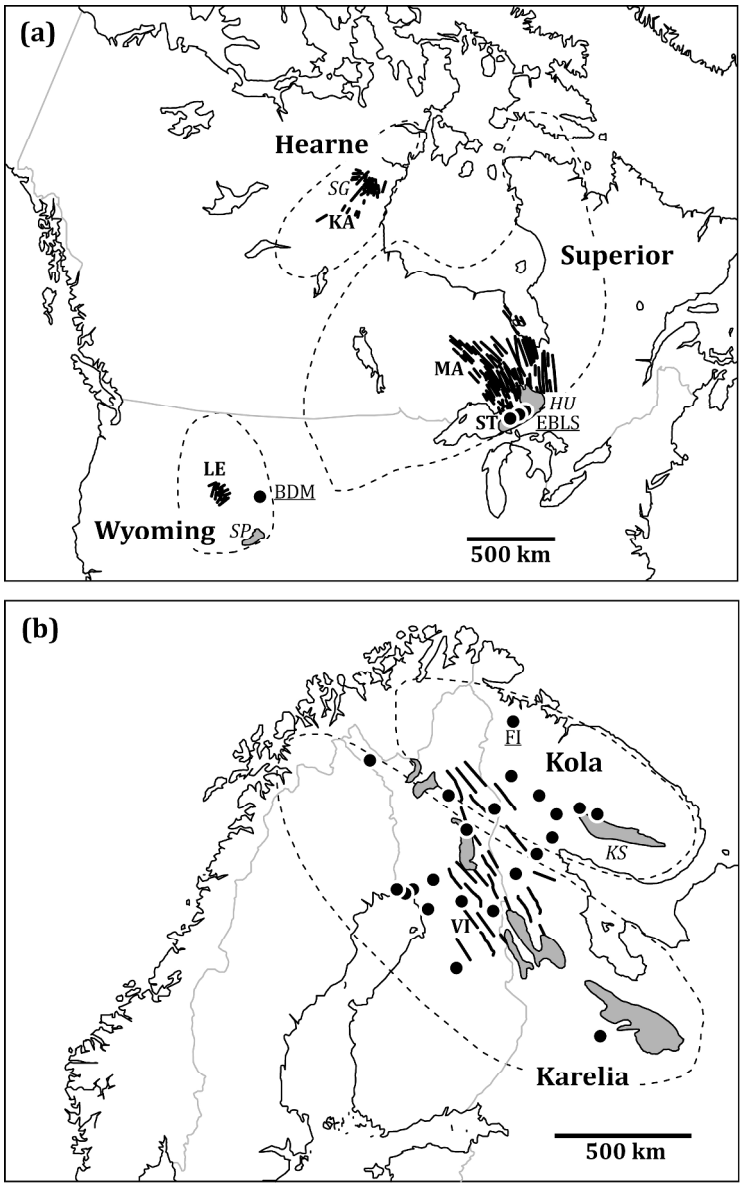

272x443mm (300 x 300 DPI)

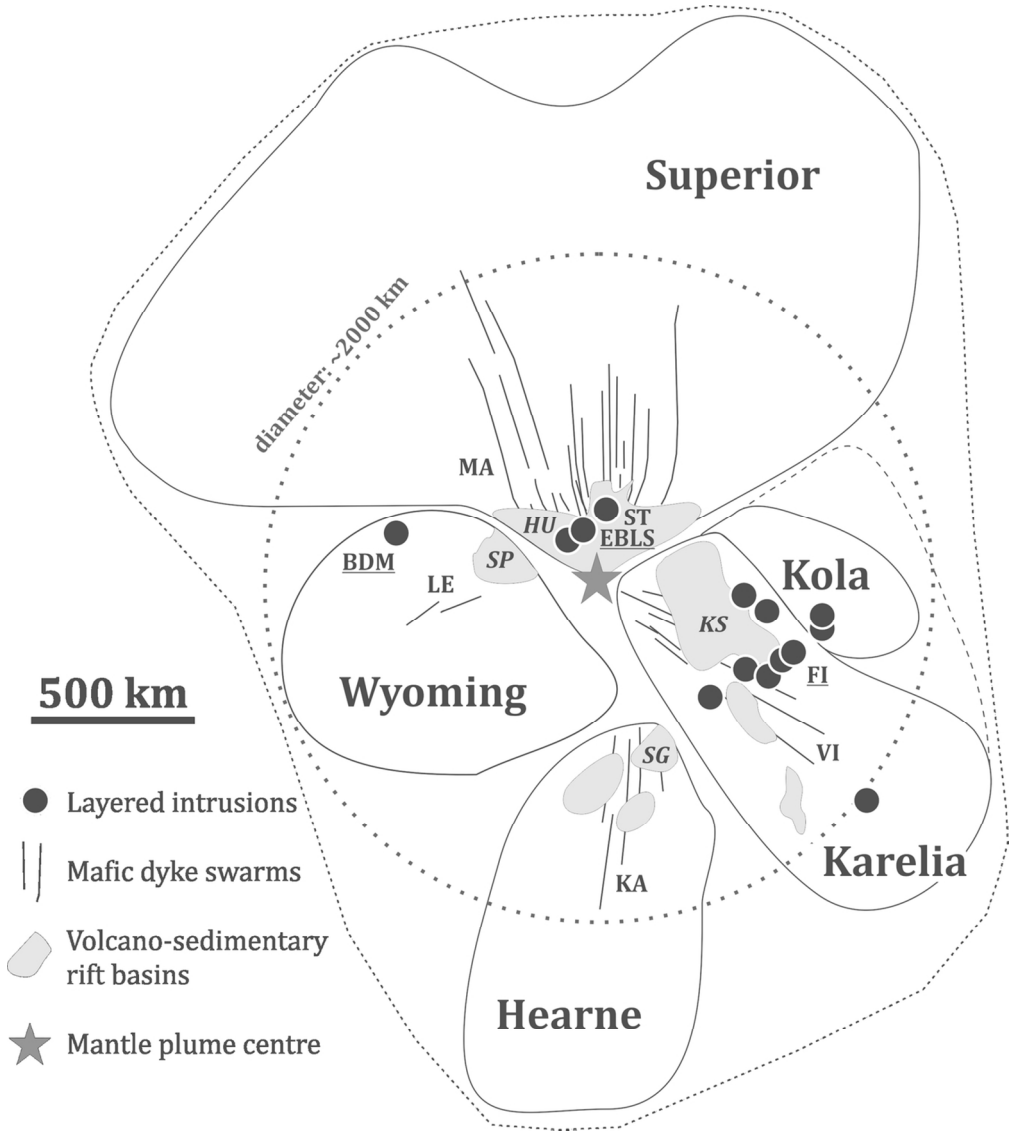

113x127mm (300 x 300 DPI)

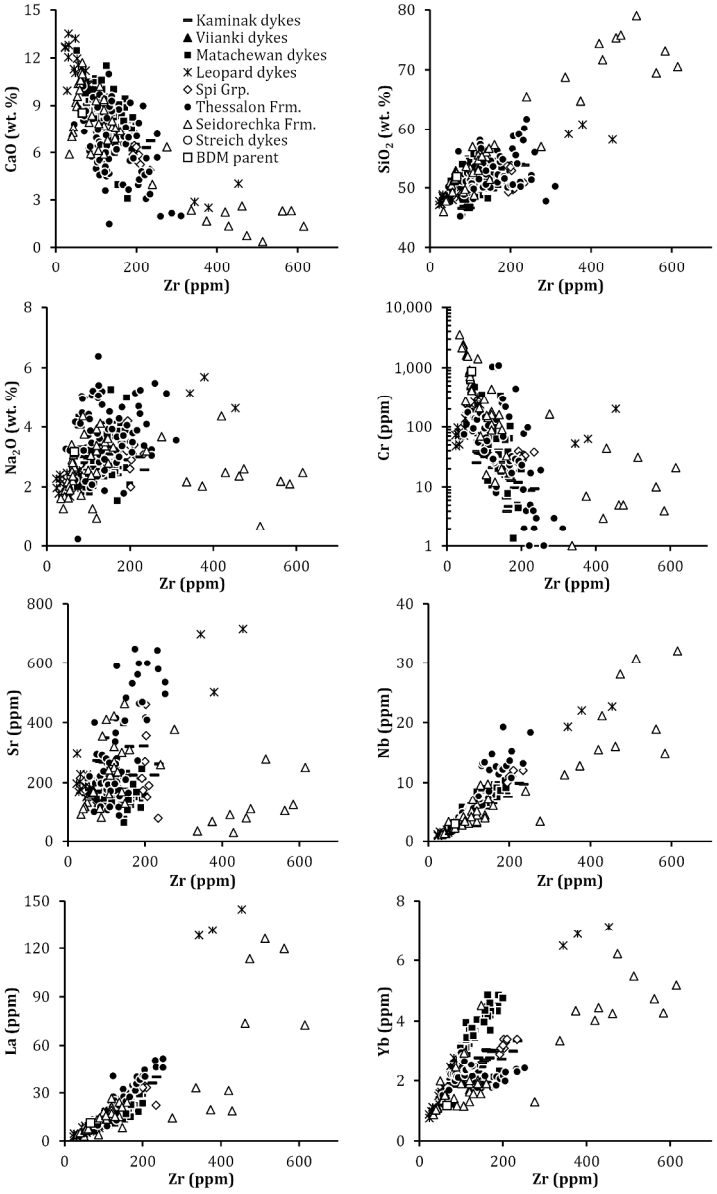

299x497mm (300 x 300 DPI)

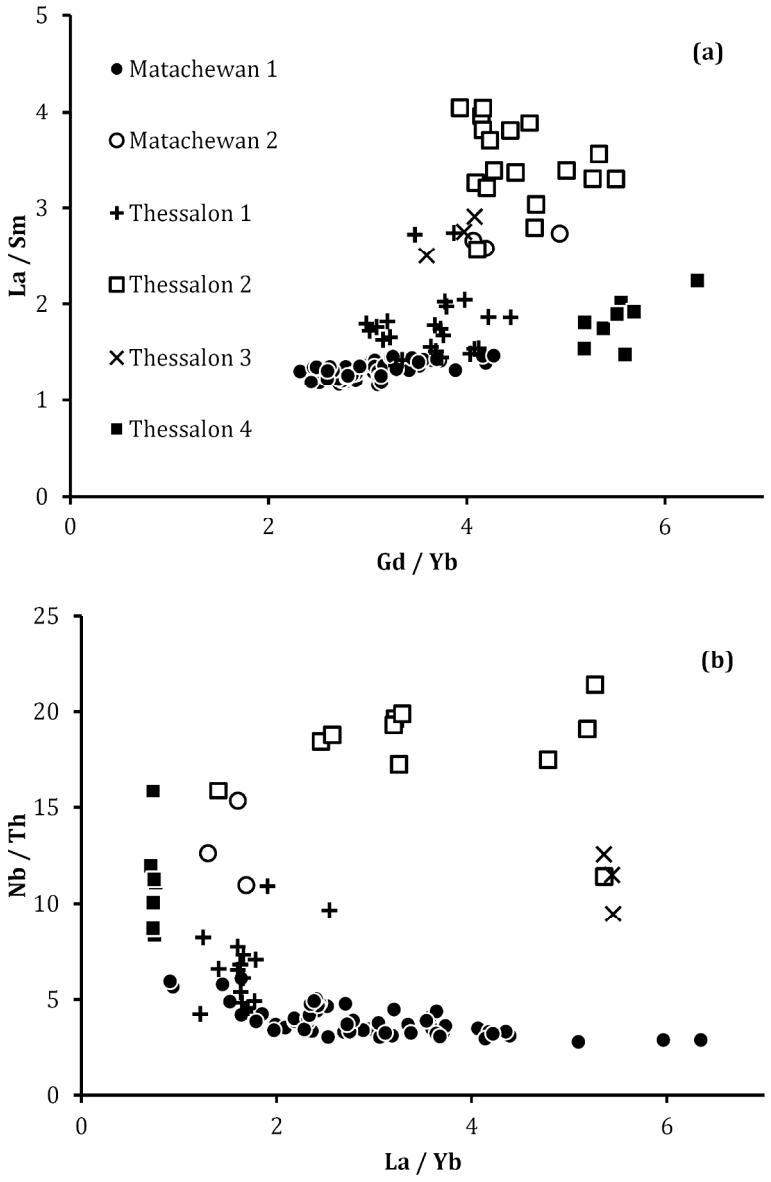

305x467mm (300 x 300 DPI)

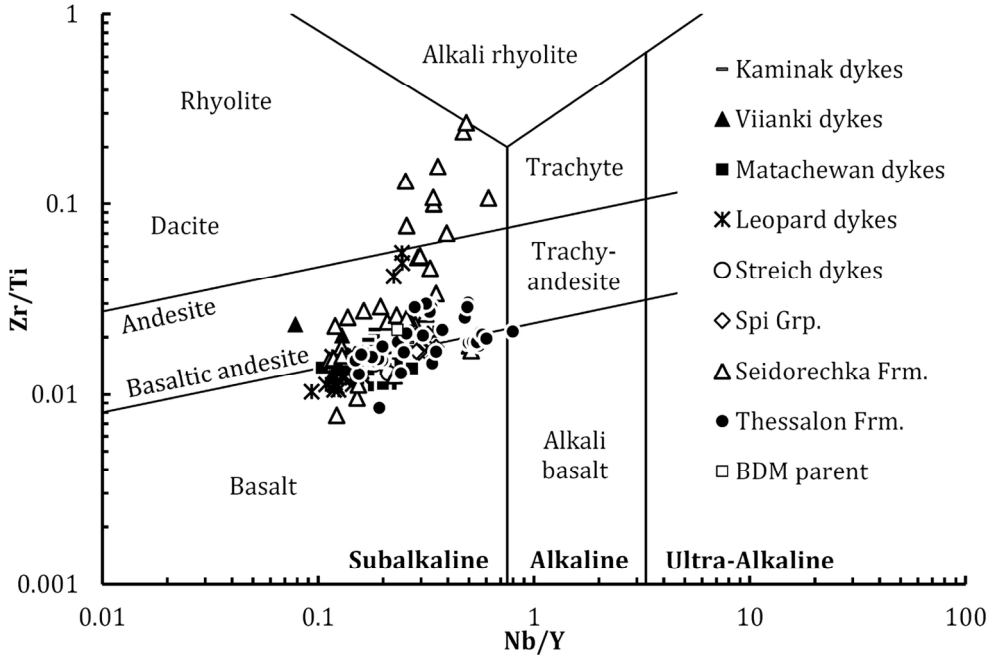

135x91mm (300 x 300 DPI)

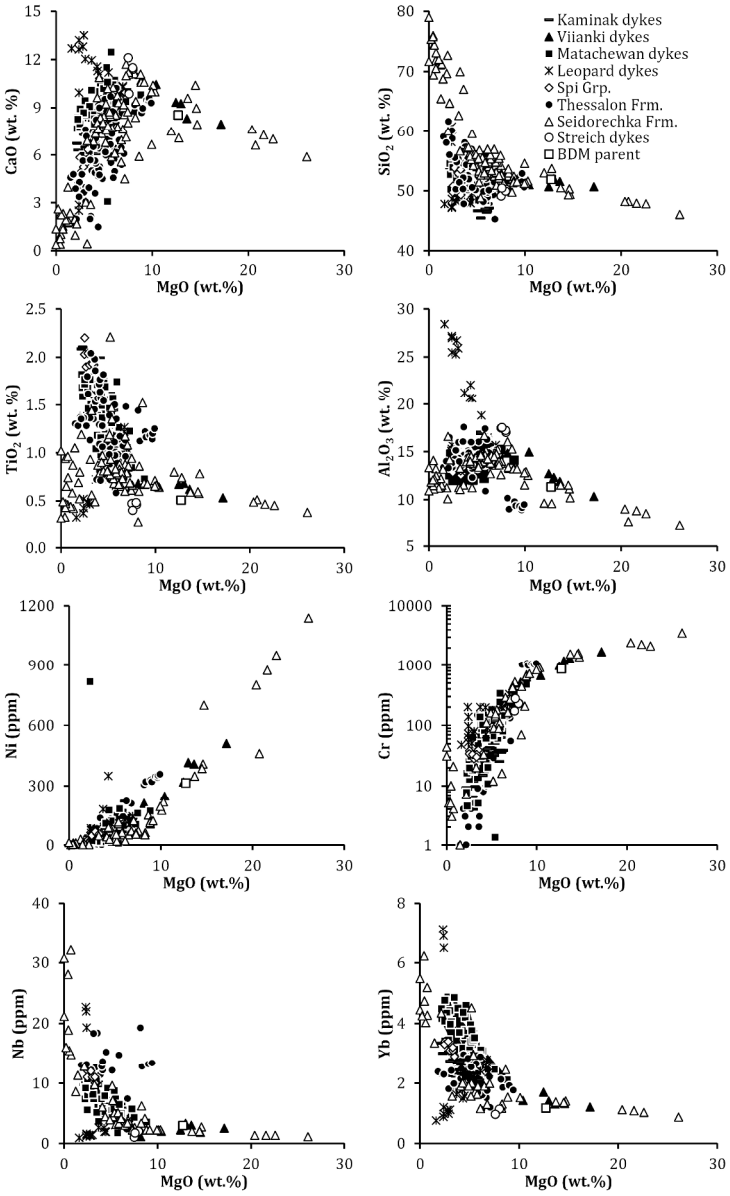

294x480mm (300 x 300 DPI)

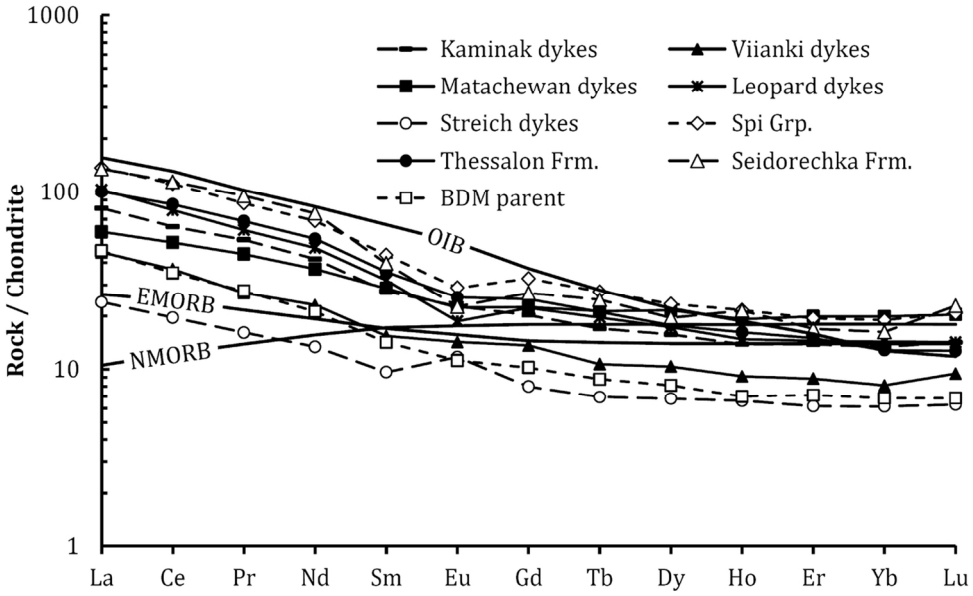

121x73mm (300 x 300 DPI)

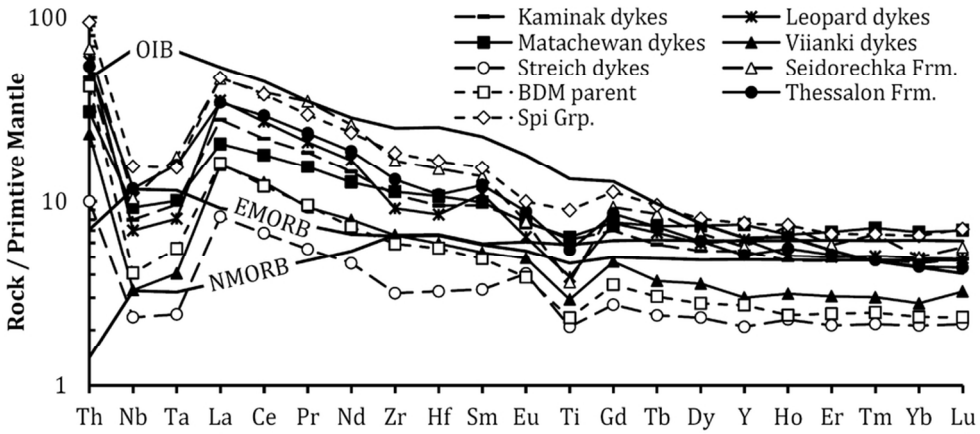

90x40mm (300 x 300 DPI)

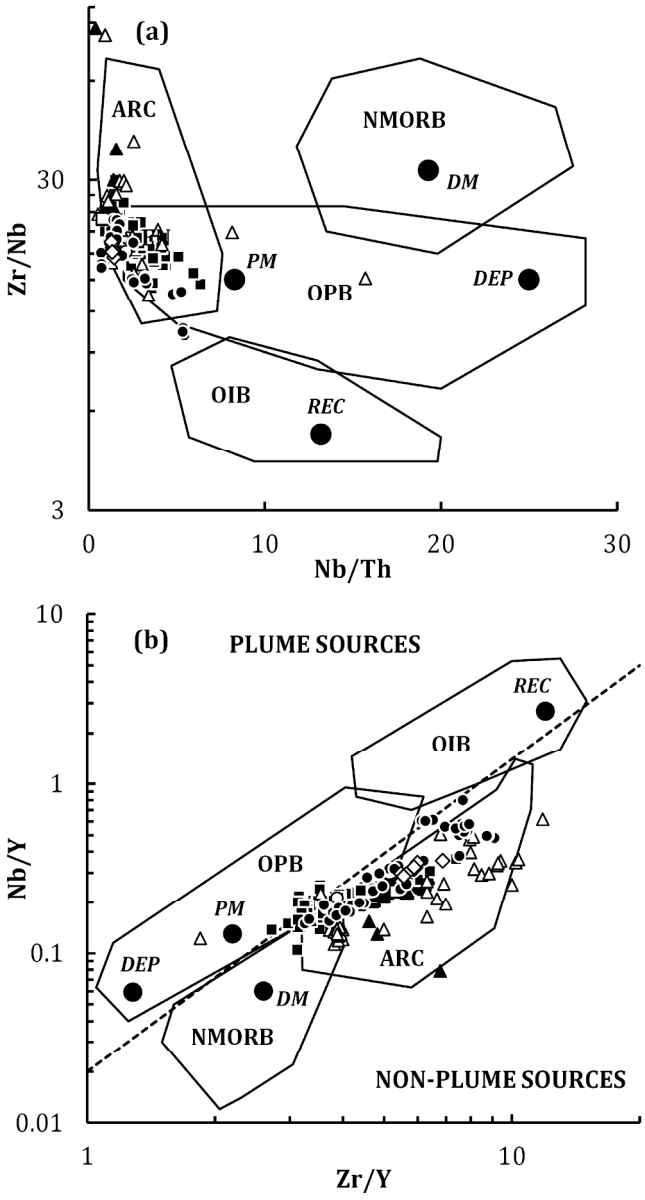

366x670mm (300 x 300 DPI)

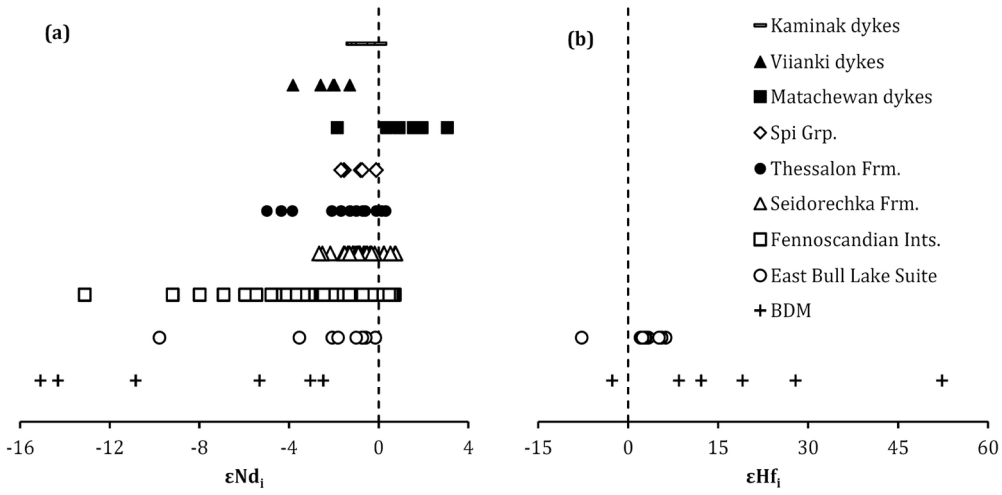

155x80mm (300 x 300 DPI)

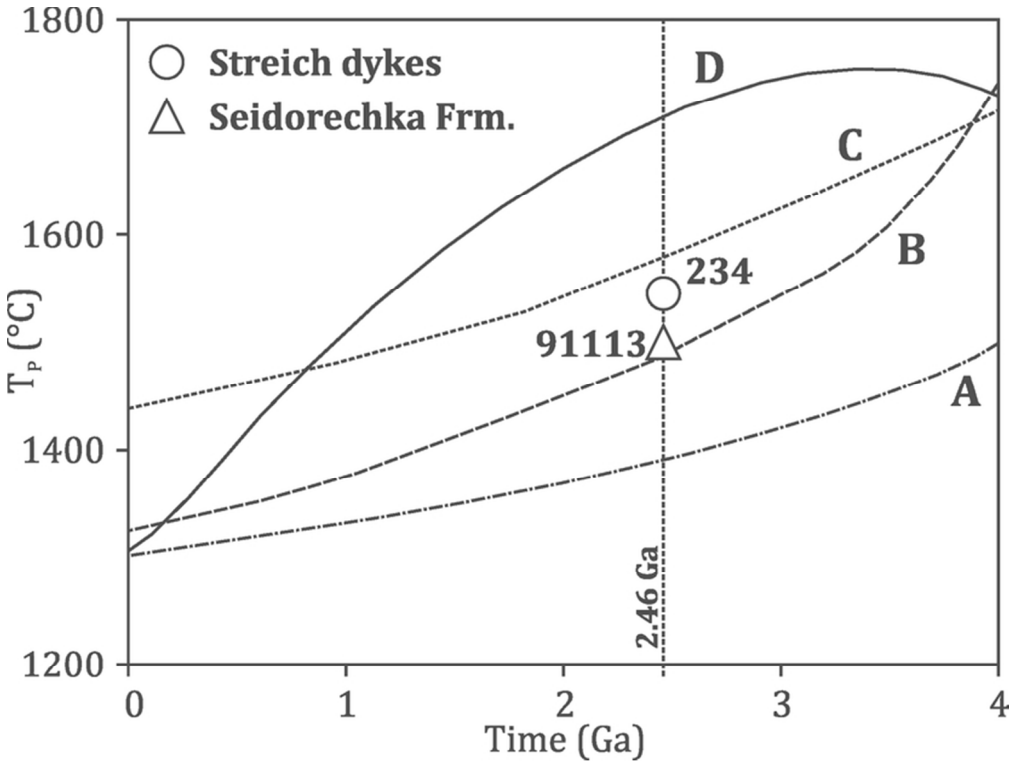

70x52mm (300 x 300 DPI)

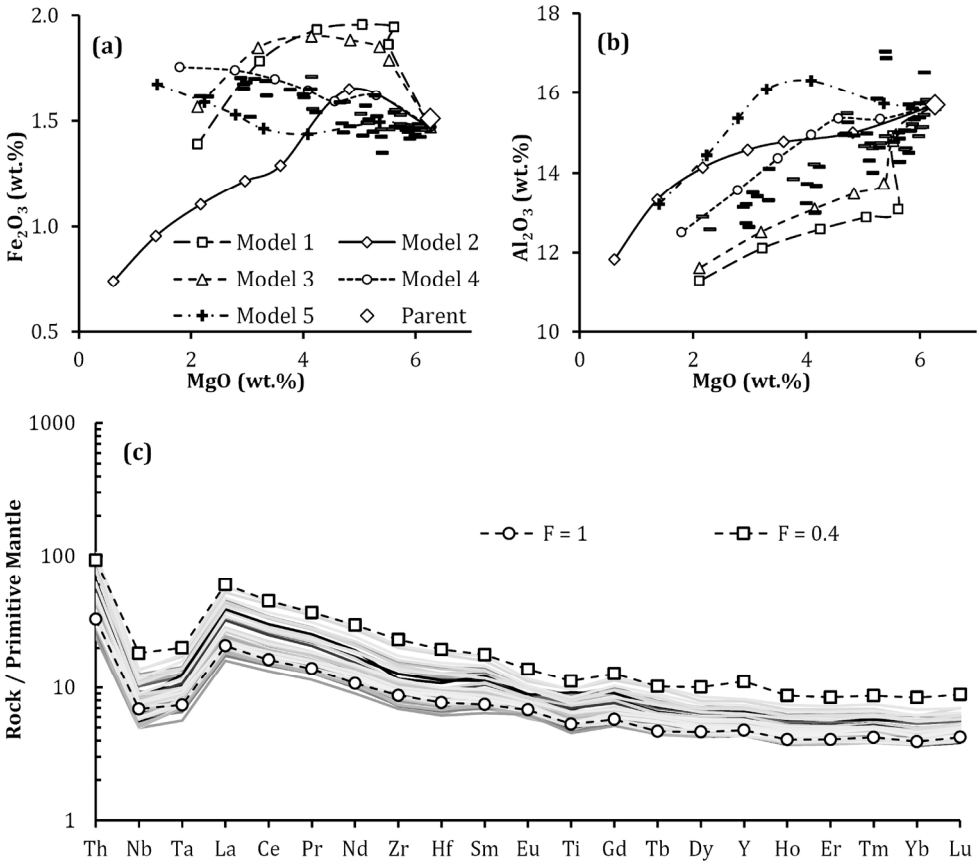

175x153mm (300 x 300 DPI)

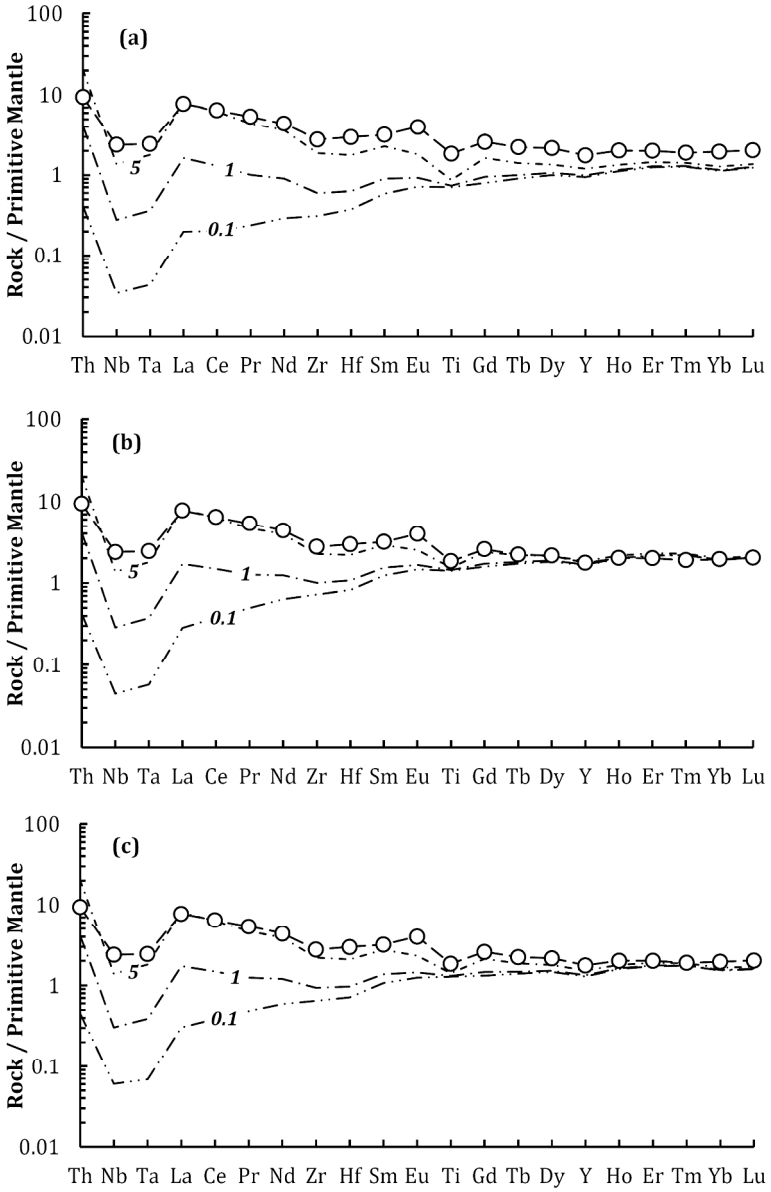

304x464mm (300 x 300 DPI)

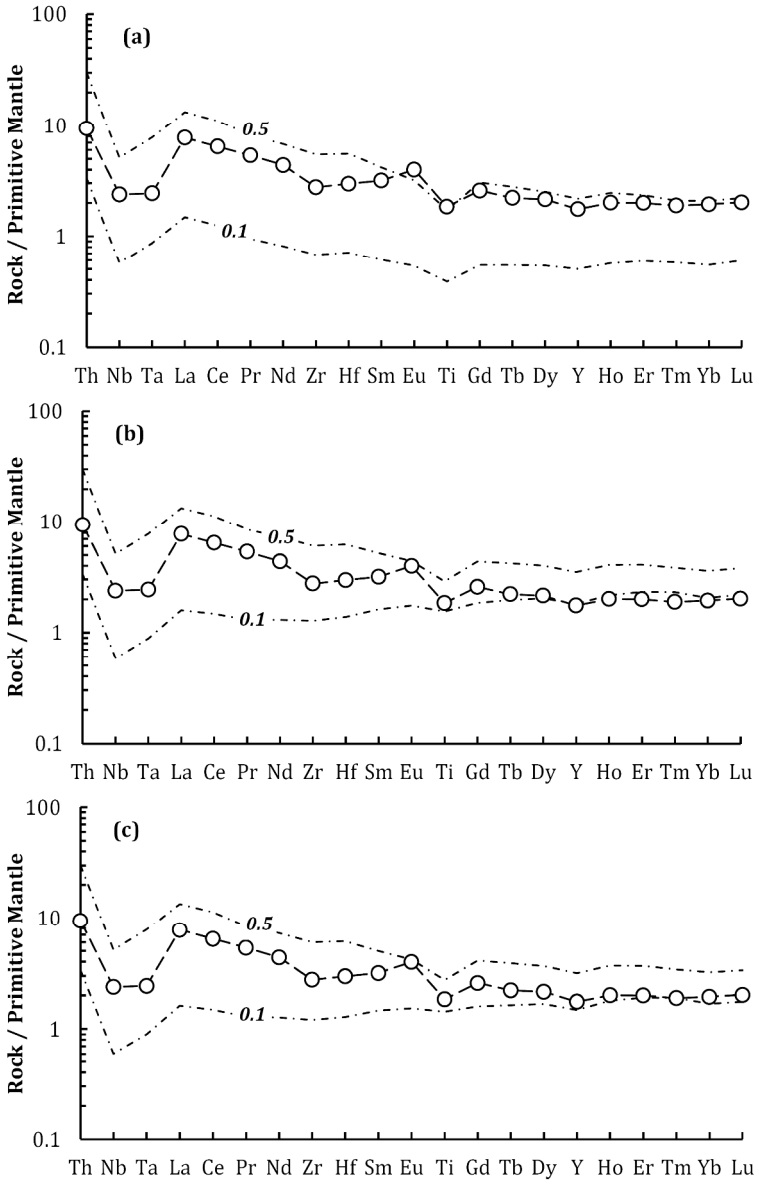

312x488mm (300 x 300 DPI)

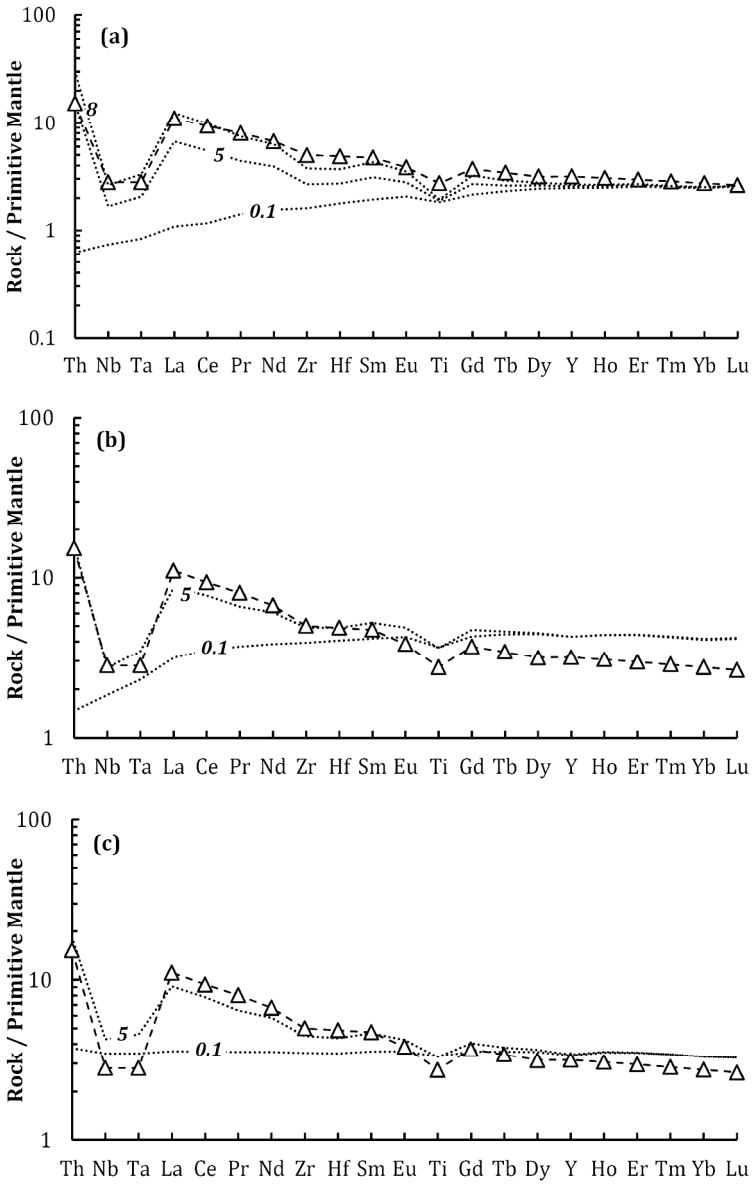

315x496mm (300 x 300 DPI)

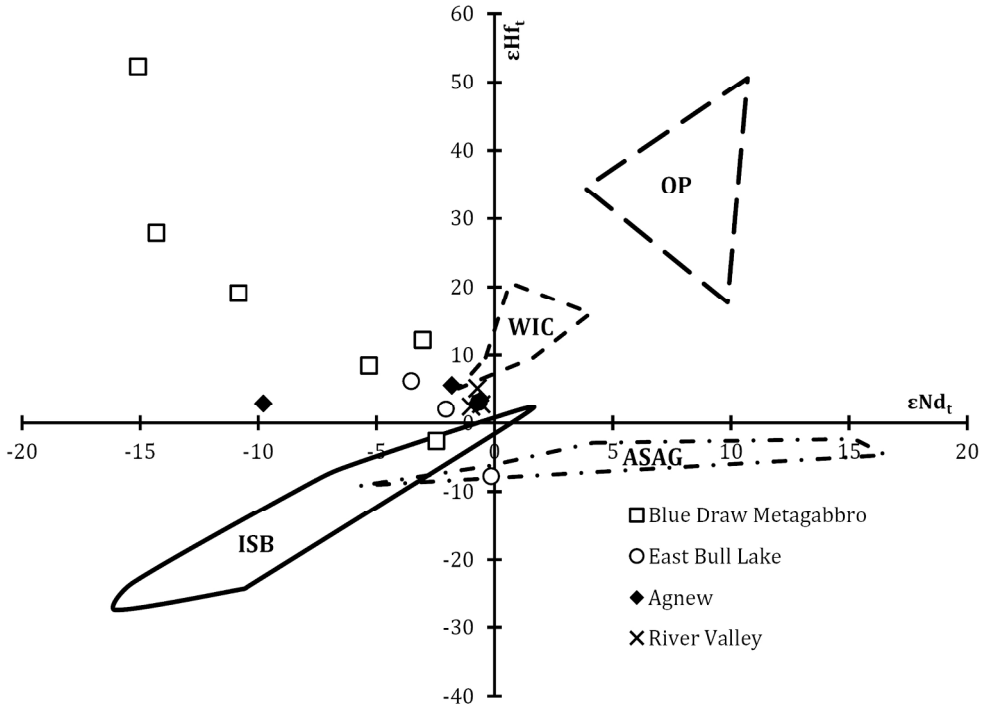

222x164mm (300 x 300 DPI)

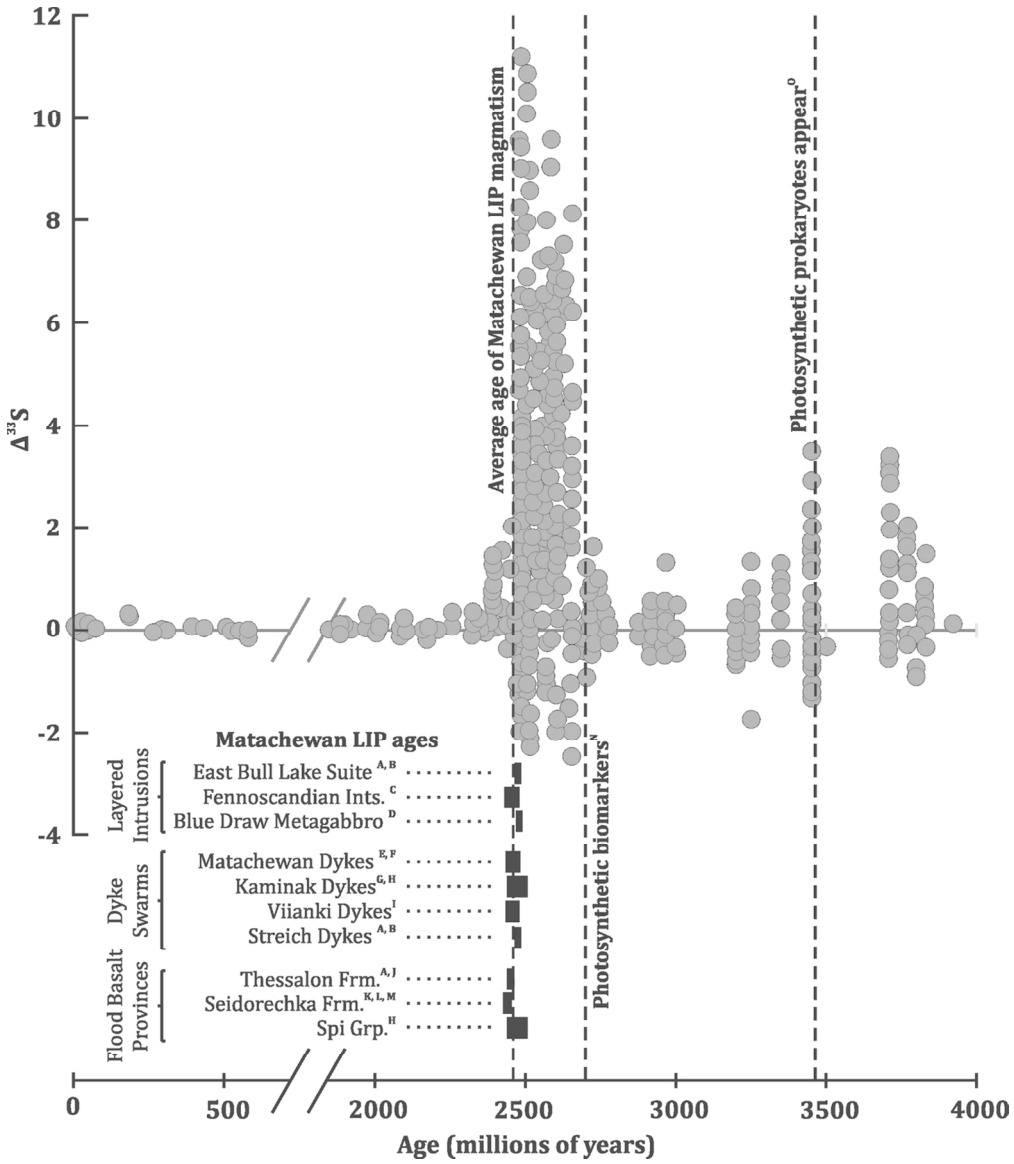

113x130mm (300 x 300 DPI)